GEOPHYSICS, VOL. 70, NO. 5 (SEPTEMBER-OCTOBER 2005); P. 3SO–28SO, 32 FIGS.
10.1190/1.2098670

75th Anniversary

Seismic attributes — A historical perspective

by Satinder Chopra[1] and Kurt J. Marfurt[2]

ABSTRACT

A seismic attribute is a quantitative measure of a seismic characteristic of interest. Analysis of attributes has been integral to reflection seismic interpretation since the 1930s when geophysicists started to pick traveltimes to coherent reflections on seismic field records. There are now more than 50 distinct seismic attributes calculated from seismic data and applied to the interpretation of geologic structure, stratigraphy, and rock/pore fluid properties. The evolution of seismic attributes is closely linked to advances in computer technology. As examples, the advent of digital recording in the 1960s produced improved measurements of seismic amplitude and pointed out the correlation between hydrocarbon pore fluids and strong amplitudes ("bright spots"). The introduction of color printers in the early 1970s allowed color displays of reflection strength, frequency, phase, and interval velocity to be overlain routinely on black-and-white seismic records. Interpretation workstations in the 1980s provided interpreters with the ability to interact quickly with data to change scales and colors and to easily integrate seismic traces with other information such as well logs. Today, very powerful computer workstations capable of integrating large volumes of diverse data and calculating numerous seismic attributes are a routine tool used by seismic interpreters seeking geologic and reservoir engineering information from seismic data. In this review paper celebrating the 75th anniversary of the Society of Exploration Geophysicists, we reconstruct the key historical events that have lead to modern seismic attribute analysis.

INTRODUCTION

The goal of seismic exploration is to map geologic features associated with hydrocarbon deposition, generation, migration, and entrapment. The goal of seismic exploitation is to characterize the static and dynamic characteristics of subsurface reservoirs. Cosentino (2001) lists these parameters as structure (horizon depth, reservoir thickness, faults, etc.), internal architecture (heterogeneity), petrophysical properties (porosity, permeability, etc.) and hydrocarbon properties (product, thermodynamics, etc.). Conventional logging programs provide sparsely sampled one-dimensional (or "vertical") measurements; indeed, many of the above properties are not measured at all in a well but need to be estimated. A good seismic attribute either is directly sensitive to the desired geologic feature or reservoir property of interest or allows us to define the structural or depositional environment and thereby to infer some feature or properties of interest. While bright spots (high reflectivity) are an obvious example of an attribute that is directly related to a parameter of interest, the inference

Manuscript received by the Editor March 14, 2005; revised manuscript received April 7, 2005; published online September 14, 2005.
[1]Arcis Corporation, Reservoir Services, Calgary, Alberta T2P 3Y6, Canada. E-mail: schopra@arcis.com.
[2]Allied Geophysical Laboratories, University of Houston, Houston, Texas 77204-5006. E-mail: kmarfurt@uh.edu.

of structure or stratigraphy began with the first reflection seismology recordings in the 1930s. The first attribute is simply the picked two-way traveltime of a reflection event.

After scanning through his or her data, a skilled seismic interpreter develops one or more geologic hypotheses on which to identify leads and build plays. While science (particularly that based on geologic principles) plays a role, much of the actual identification of features is done by comparing them to a mental database of examples. Many would define seismic interpretation to be a mix of art and science. Once an interpreter has identified a seismic feature or pattern that is associated with successful wells (whether the scientific underpinning is valid or not!), he or she can rapidly find more of the same. This pattern recognition by experienced interpreters is mind-boggling to younger geophysicists who often come armed with a great deal more formal mathematics.

One of the goals of seismic attributes is to somehow capture this expertise by quantifying the amplitude and morphological features seen in the seismic data through a suite of deterministic calculations performed on a computer. For instance, the coherence attribute developed in the mid-1990s captures the same discontinuities seen in the seismic data and interpreted as faults by workers such as Rummerfeld (1954) some 40 years earlier.

Many modern techniques make simultaneous use of multiple attributes. In selecting the appropriate multiple attributes, Barnes (2000) advises that we use attributes that are independent of one another. Kalkomey (1997) warns that in order to avoid false positive correlations, we should only use those attributes that are associated with physical properties and features of interest to our play or reservoir. Bob Sheriff (personal communication, 2005) laments "mindless interpretation" where geoscientists search through a suite of attributes and stop when they find one that shows a feature they want to see. If possible, we recommend that each attribute capture only one type of physical property or feature, which can then be combined intelligently through geostatistics or other multi-attribute analysis tools.

In the most general sense, the definition of seismic attributes encompasses all quantities derived from seismic data; thus, we consider interval velocity, inversion for acoustic impedance, pore pressure prediction, reflector terminations, as well as complex-trace attributes and amplitude variation with offset (AVO) to be attributes. By assigning the name attribute to a quantity based on very sophisticated calculations such as impedance inversion and pore pressure prediction, we recognize that these estimates are somehow contaminated by errors and, thus, require calibration to well data via geostatistics or other data integration techniques.

Classification of attributes

As seismic attributes grew in both their number and variety over the last three decades, many authors have attempted to classify them into families, with the ultimate goal of better understanding and application. To put this growth in perspective, Bob Sheriff's 1984, 1991, and 2002 editions of his encyclopedic dictionary of geophysics contain the following entries on attributes: The 1984 edition devoted 26 lines to attributes, complex trace analysis, and hydrocarbon indicators, plus a full-page figure of complex trace analysis. The 1991 edition covered the same three categories and a table of hydrocarbon indicators (Figure H-7), for a total of 48 lines plus the same full-page image of the 1984 edition. The 2002 edition contains 153 lines in all (69 lines of text, a 34-line table, 9 lines on coherence, 25 lines on hydrocarbon indicators, and 16 lines on complex trace analysis, plus 6 figures on attributes).

Taner et al. (1994) divide attributes into two general categories: geometrical and physical. The objective of geometrical attributes is to enhance the visibility of the geometrical characteristics of seismic data; they include dip, azimuth, and continuity. Physical attributes have to do with the physical parameters of the subsurface and so relate to lithology. These include amplitude, phase, and frequency. The classification may be further divided into poststack and prestack attributes. Brown (1996b, 2004) classified attributes using a tree structure with time, amplitude, frequency, and attenuation as the main branches, which further branch out into poststack and prestack categories. Time attributes provide information on structure, whereas amplitude attributes provide information on stratigraphy and reservoir. Chen and Sidney (1997) provided a classification based on wave kinematic/dynamic categories and geologic reservoir feature categories. Barnes (1997) developed a classification of complex-trace attributes depending on the relationship among different attributes and seismic data. Recognizing amplitude and phase as fundamental attributes from which all others are derived, attributes are classified as 1D, 2D, or 3D, as time or depth, and as instantaneous or local. Such classifications have been attempts at developing an intuitive understanding of the different attributes, and this has helped in the application of attributes or combinations of attributes in discriminating subsurface features.

We prefer Liner et al.'s (2004) classification into general and specific categories. Liner et al.'s general attributes are measures of geometric, kinematic, dynamic, or statistical features derived from seismic data. They include reflector amplitude, reflector time, reflector dip and azimuth, complex amplitude and frequency, generalized Hilbert attributes, illumination, edge detection/coherence, AVO, and spectral decomposition. These general attributes are based on either the physical or morphological character of the data tied to lithology or geology and are therefore generally applicable from basin to basin around the world. In contrast, specific attributes have a less well-defined basis in physics or geology. While a given specific attribute may be well correlated to a geologic feature or to reservoir productivity within a given basin, these correlations do not in general carry over to a different basin. There are literally hundreds of specific attributes. We add a third category to Liner et al.'s classification, that of "composite" attributes [also called meta attributes by Meldahl et al. (2001)]. Many of the specific attributes cited in the literature are sums, products, or other combinations of more fundamental general attributes. We prefer two types of composite attributes: those used to display more than one attribute at a time (composite displays discussed under "The rise of seismic attributes") and those combined using geostatistics, neural nets, or other classification technology [such as Meldahl et al.'s (2001) meta attributes]. Given the dangers of false correlations, we prefer when possible to use attributes that individually correlate to only one physical or geologic variables of interest, followed by geostatistics, neural networks, clustering, or visualization to combine multiple attributes in a meaningful manner.

Outline of this review paper

In this fifth of a suite of ten papers celebrating the 75th anniversary of the Society of Exploration Geophysicists, we attempt to reconstruct the key historical events that lead to modern seismic attribute analysis tools and workflows (Figure 1). While the foundations of attribute analysis evolved during the development of seismic exploration, attribute analysis, as we now know it, had to wait until modern digital recording. We do not feel we have the proper perspective to cover the most recent developments, including volumetric estimation of Q, volumetric curvature, and prestack attributes. We also do not cover the extensive literature on AVO attributes, which we feel will be better covered in a paper addressing rock physics. Geostatistics and multiattribute classification also would require a paper as long as this.

1950–1960

Attributes from analog data

Some of the most important seismic attributes appeared long before digital recording, during the time of paper records. Roy Lindseth (2005) remembers the early 1950s as the time when reflections were inked by hand on seismic records, and reflections were graded by labels in terms of consistency and character. Zones of no reflection would be labeled *NR* to signify recordings so poor that reflections could not be distinguished from the unruly background noise. Lindseth (2005, 16) remarks that "demonstrating the true doodlebug spirit of turning adversity into advantage, Ben Rummerfeld (1954) correctly predicted in one area that *NR* gaps correspond to faulting. This predecessor of semblance was perhaps the first documented use of seismic attributes to find oil."

Nigel Anstey (2005) recollects that the main reason for adopting magnetic analog recording in 1954 was to provide frequency analysis for optimization of filter settings. Later, a more important benefit emerged — reproducible recording allowed corrected cross sections. This was a significant development at the time, in that the structure could be seen directly from seismic wiggles. It was a new experience, and the geologists were impressed! Bob Sheriff (personal communication, 2005) doesn't disagree with this technical advantage, but remembers the justification of magnetic recording to his company's management was the ability to evaluate alternative analog filters and mixing on the field records, rather than embedding it directly in the recording process. Reflector picks were made manually, transferred to a map, and hand contoured in order to evaluate closure about potential hydrocarbon traps. During the same time period, maps of reflector dip were commonly created. Isochors (time-thickness maps) were calculated directly from the seismic data or, occasionally, computed from the mapped horizons. Faults were recognized by discontinuities and (more commonly) the presence of diffractions and also posted on maps, but the correlations between lines was a source of error. While tedious to generate, these measurements were clearly attributes of the seismic data. While all four of these attributes (structural elevation, dip, thickness, and discontinuities) have been greatly improved with the advent of digital data, one of the most important attributes — amplitude — had to wait for digital recording and would not appear until 1972.

1960–1970

Digital recording and bright-spot detection

Until 1963, explorationists relied on inaccurate, low-resolution analog data in planning their exploration investments. Nigel Anstey (2005) recalls that in the mid-1960s, with useful contributions pouring in from Milo Backus and Bill

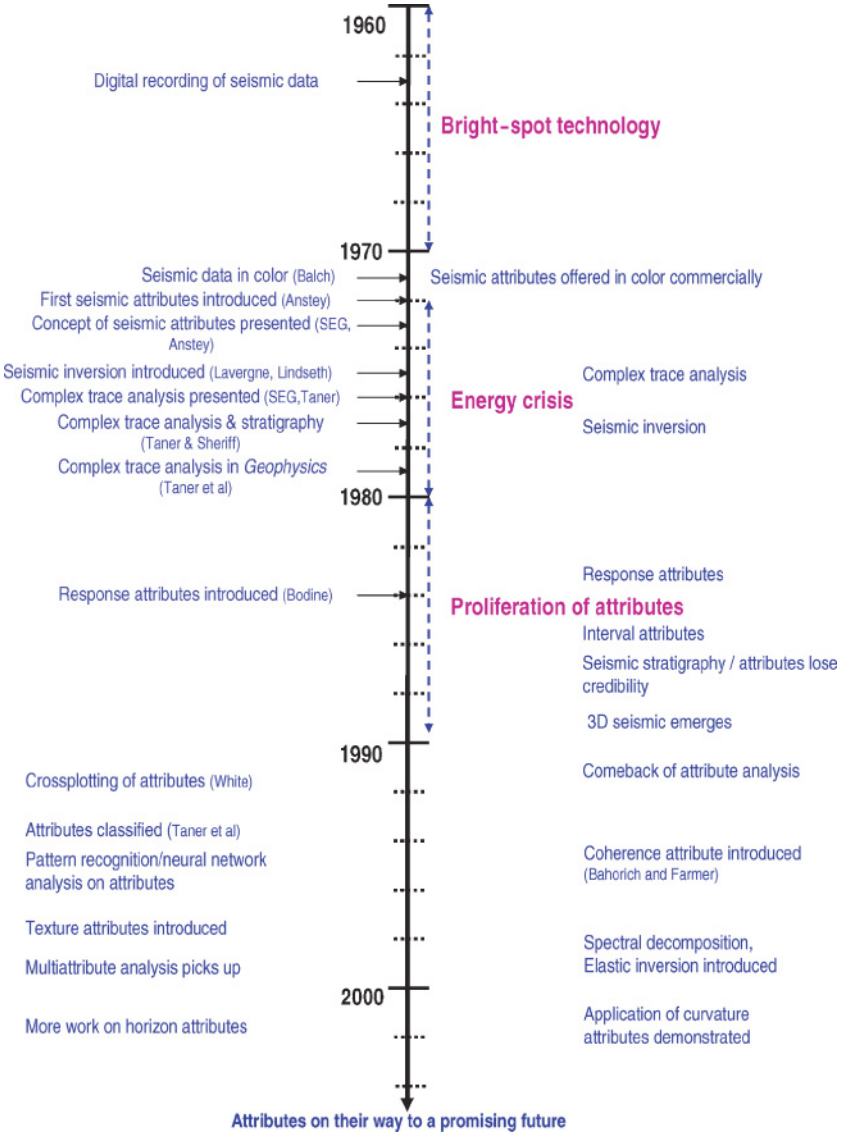

Figure 1. A time line of seismic attribute developments and their relation to key advances in seismic exploration technology. (Modified from Barnes, 2001.)

Schneider and the development of the velocity spectrum by Tury Taner and Fulton Koehler, multifold data began to help with the interval velocity computations. Bob Sheriff (personal communication, 2005) recalls interval velocity estimation as a serendipitous by-product of the original goal of producing seismically derived time-to-depth conversion. In the context of Peterson et al.'s (1955) synthetic seismogram and its implied convolutional model, velocity is arguably the most basic of attributes. By the late 1960s, a few geophysicists had started noticing the strong isolated reflections and changes in reflection character on seismic sections, which in 1975 would form the foundation of seismic stratigraphy based on onlap, offlap, and other morphological patterns (Forrest, 2000). Initially, it was thought that some of these reflections were caused by "hard streaks," and people were skeptical that these observations were meaningful. But gradually, when some of these strong events encountered gas zones on drilling, interpreters started taking them seriously. These streaks of high amplitudes seen on seismic sections were christened bright spots and gave birth to bright-spot technology.

Searches of worldwide technical literature of the time revealed that some research papers (Churlin and Sergeyev, 1963) had already reported direct detection of hydrocarbons by seismic means. This search revealed concerted efforts in carrying out correlation studies of bright spots with well data and field studies. It was found that reflections from gas-charged reservoir rocks showed much larger amplitudes than reflections from adjacent oil- or water-saturated zones. Bob Sheriff (personal communication, 2005) recalls that no one was interested in finding gas during this period — bright spots were misinterpreted and sold as a means of finding the associated oil. It was only later that we realized that these bright spots were attributable to gas, or the effect of gas dissolved in oil, causing a low-impedance anomaly. Even if initially poorly understood, the revelation that anomalously higher-amplitude seismic events in young clastic basins could indicate hydrocarbons gave a new level of importance to the seismic exploration method. By 1970, oil companies were successfully using bright-spot phenomena to identify gas-saturated reservoirs (Forrest, 2000).

By using a long-window automatic gain control (AGC), the high-amplitude anomalies associated with hydrocarbon accumulations became more obvious but, whereas some were then visible, some of the detailed structural information was lost. Thus, usually two sections were plotted: a bright-spot section and a conventional section (Anstey, 2005).

Digital recording greatly improved the quality of seismic data, and by 1975, nearly all seismic recording was digital. With digital recording came the awareness of preserving relative amplitudes. After early successes, bright-spot technology rapidly evolved in the early 1970s, including efforts to quantify seismic amplitude changes and to calculate pay-sand thicknesses. The application of this technology had a major impact on bidding in the offshore Louisiana shelf and the Gulf Mexico. Along with time/structure and velocity, seismic amplitude is the most important attribute in use today.

Bright-spot technology included more than high amplitudes; it also included flat spots, frequency loss, time sags, time shadows, polarity reversals, and dim spots — features identified by the interpreter that would form the motivation for later seismic-attribute developments. Encouraged by the success of the application of bright-spot technology, especially for reducing risk in high-cost environments, geophysicists now started looking at these other hydrocarbon indicators. Taner et al. (1979) observed low-frequency shadows below hydrocarbon reservoirs (which we now know to be caused by gas sands and condensates). No definitive explanation was provided to explain this phenomenon, although several possible contributing reasons were proposed, nor has much has been published on this topic since. [Recently, Ebrom (2004) listed at least ten mutually nonexclusive mechanisms for this effect.] The ancient low-frequency shadows are an indication of the seismic attenuating properties of gas-filled rock and currently are receiving attention with the development of Q attributes.

Reflector dip

While binary-gain digital recording inspired amplitude-analysis techniques, it also enabled developers to improve structural interpretation techniques. Picou and Utzman (1962) used a 2D unnormalized crosscorrelation scan over candidate dips on 2D seismic lines to estimate dip at every sample and every trace on a seismic section (Figure 2). The result of this process was a suite of dip vectors, which was plotted on the seismic section using specialized hardware. An earlier method of dip-scanning using crosscorrelation, developed by MIT's. Geophysical Analysis Group (GAG), was later published by Simpson et al. (1967). Further work on estimating reflector dip was driven by contemporaneous developments in map migration, which is summarized by Bednar's (2005) 75th Anniversary review paper on seismic migration. As shown by these examples, the computer was being used as a means of automatically extracting additional information from the recorded seismic data.

1970–1980

Introduction of color in seismic displays

In 1971, A. H. Balch developed a computer-graphic-photographic system called the color sonogram to display the frequency spectra of seismic events simultaneously with their time-varying waveforms. In this display, the waveforms are displayed using a conventional variable-area scheme but with the positive lobe now colored to represent the frequency component of the data. The lateral changes in rock attenuation, or the loss of high frequencies caused by slight lateral changes in move-out velocity, etc., could show up as color shifts on such displays. Balch's (1971) paper is credited with being the first published in GEOPHYSICS to display seismic data in color. His work heralded the beginning of an era where color, with the enhanced dynamic range it offers, was used for meaningful analysis of seismic data.

The rise of seismic attributes

At around the same time (1968–1969), Nigel Anstey at Seiscom Ltd. was working on innovative seismic displays and playing a key role in introducing color on seismic sections. Experimenting with the first gray-scale laser plotter (developed by Southwestern Industrial Electronics) installed in Seicom's office in London, Anstey and his team (Ron O'Doherty, Peter Ferrer, Judy Farrell, and later Lloyd Chapman) developed

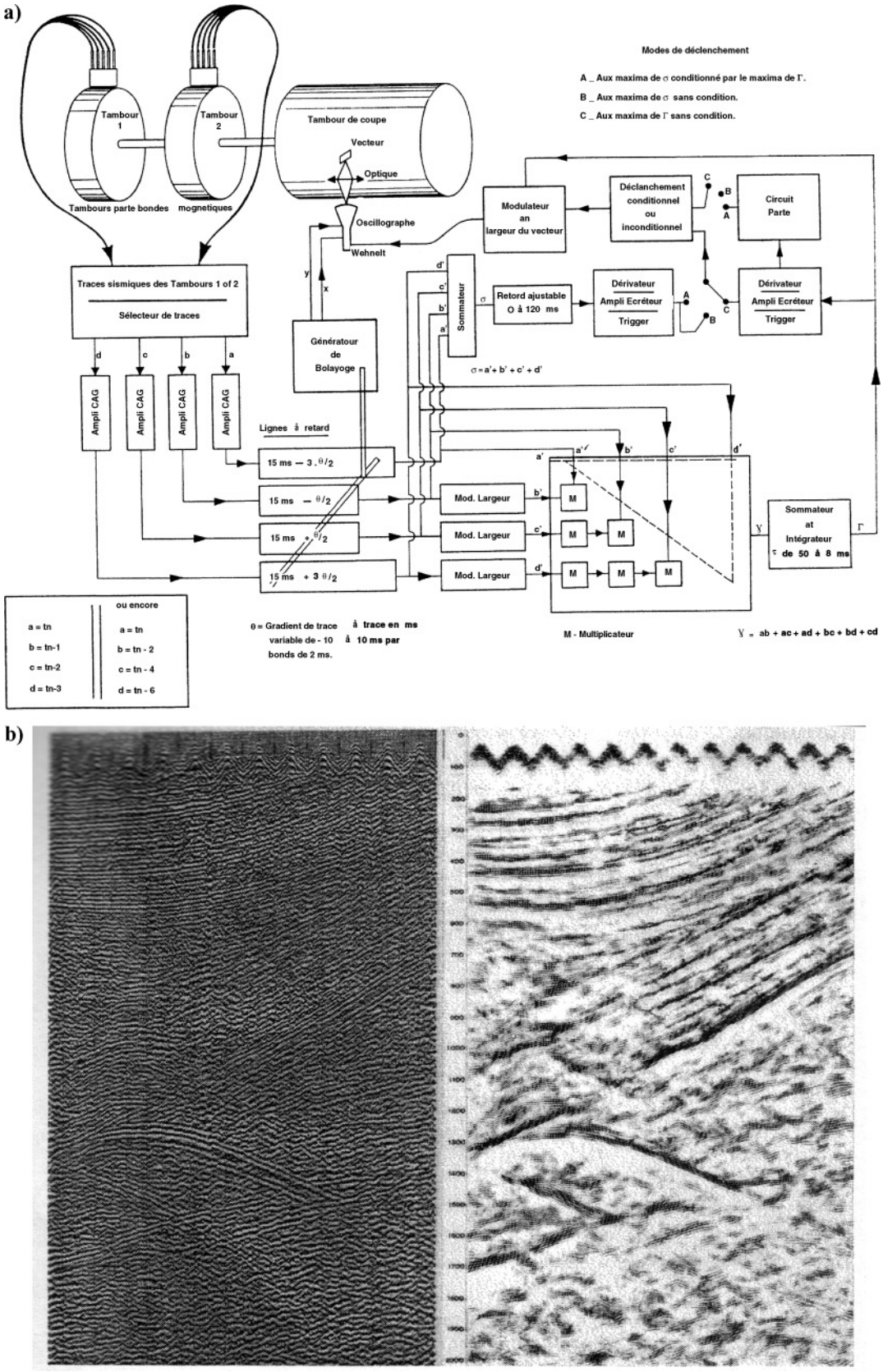

Figure 2. Perhaps the earliest example of a computer-generated seismic attribute. (a) Schematic of a device built to crosscorrelate seismic traces recorded on analog magnetic tape, which was then used to display (b) reflector dip and continuity. (After Picou and Utzman, 1962.)

color-separation techniques to display two variables on the seismic section: the normal seismic trace to give the geological picture and an auxiliary modulation in color to show interval velocity, reflection strength, frequency content, or anything else that might prove useful. The overlay of the color attributes on the black and white seismic sections resulted in displays that provided more information — the conventional black and white seismic display providing structural information and the seismic attribute overlain providing more subtle stratigraphic information. Since this was the time of the bright-spot revolution, the most popular of these displays were those of reflection strength (the amplitude of the envelope).

Anstey published his innovative work on attributes in two internal reports for Seiscom in 1972 and 1973, and also presented them at the 1973 SEG annual meeting (Anstey, 1973). The high cost of printing in those early days of color processing prevented Anstey's reports from being widely circulated. However, they do represent an important landmark for the introduction of both color and attributes into the seismic world. As Anstey puts it, "the real advance lay in the simultaneous display of an attribute in its geological context; the color was just a way of doing this" (Anstey, 2005).

In Figure 3, we display one of Seiscom Ltd.'s conventional (but still high quality) seismic displays of the early 1970s — a variable density plot of the seismic data showing the most positive values of the seismic data as black. The use of variable density (commonly called variable intensity on modern interpretation workstations) allowed interpreters to plot data in "squash-plot" form, with the horizontal scale greatly compressed, thereby emphasizing subtle structural trends. In contrast, conventional variable area plots lost progressively more dynamic range as the trace width was compressed. In Figure 4, the interval velocity, obtained using Dix's equation, is superimposed on these seismic traces. In Figures 5–9 we show several other of the earliest attribute plots: reflection strength

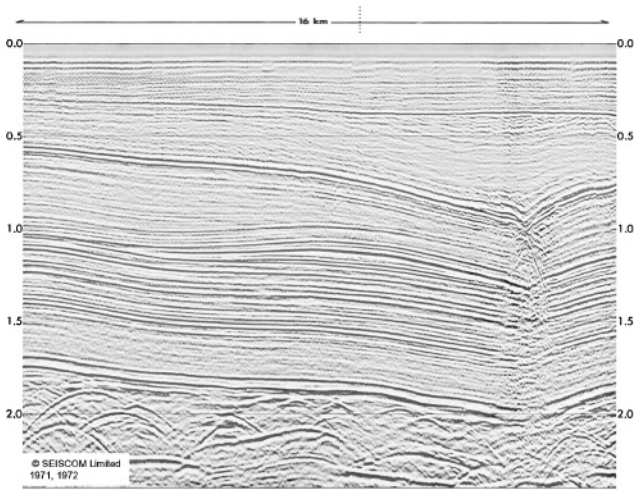

Figure 3. A state of the art seismic display from the early 1970s. The variable density plot shows strong peaks as black, zero values as gray, and strong troughs as white. Variable density allowed the compression of the horizontal scale, generating "squash plots" that enhanced subtle structure, onlap, offlap, and other stratigraphic features of interest. This image is the substrate for attribute images plotted in color in Figures 4–7. (After Anstey, 2005.)

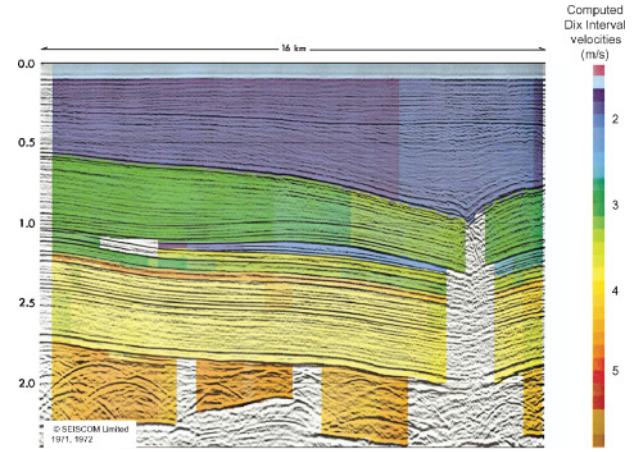

Figure 4. A composite attribute image from the early 1970s showing interval velocities (estimated using Dix's equation) superimposed on the structural section of Figure 3. (After Anstey, 2005.)

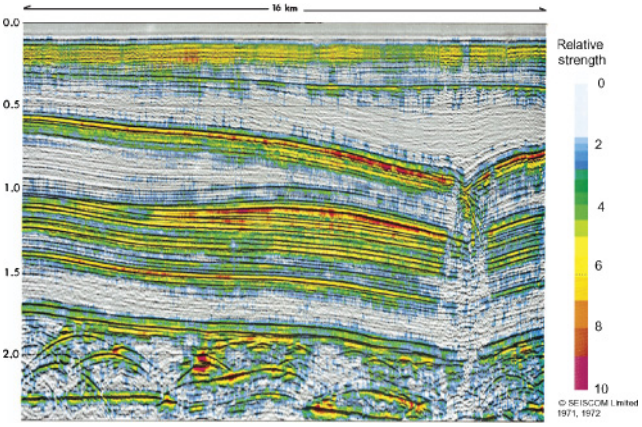

Figure 5. A composite attribute image from the early 1970s showing reflection strength (in early days, the most popular attribute) superimposed on the structural section of Figure 3. (After Anstey, 2005.)

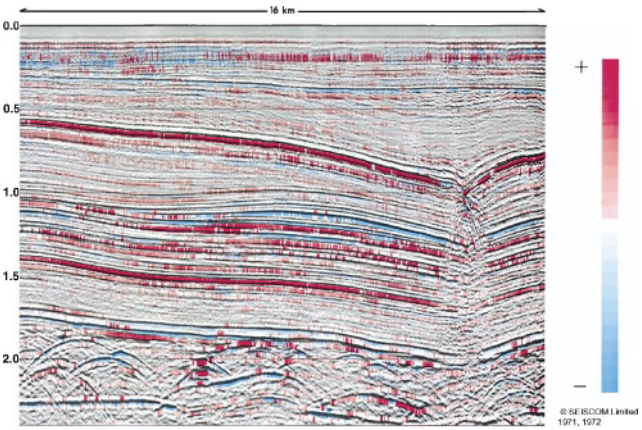

Figure 6. A composite attribute image from the early 1970s showing the apparent polarity of reflections (positive as red, negative as blue) superimposed on the structural section of Figure 3. (After Anstey, 2005.)

(Figures 5 and 8), apparent polarity (Figure 6), and high-frequency loss (Figure 7). Figure 9 shows reflection strength displays from a 2D grid of data, combined to form an isometric fence diagram. The displays could be rotated to optimize the view, "sculpted" down to reservoir level, and supplemented by a superposed contour map (Anstey, 2005).

Complex-trace analysis

After Anstey left Seiscom in 1975, two of his colleagues at Seiscom in Houston, Turhan Taner and Fulton Koehler, advanced these developments, and gave them a sound mathematical basis. Turning their attention to seismic wave propagation, they interpreted the recorded seismic waveform on geophones sensitive to particle velocity to be proportional to the kinetic energy component of the total energy flux. Under this assumption of simple harmonic motion, they felt it should be possible to compute the potential energy component as well. Thus, Koehler developed an energy-based procedure and computed the envelope of a seismic trace in this manner.

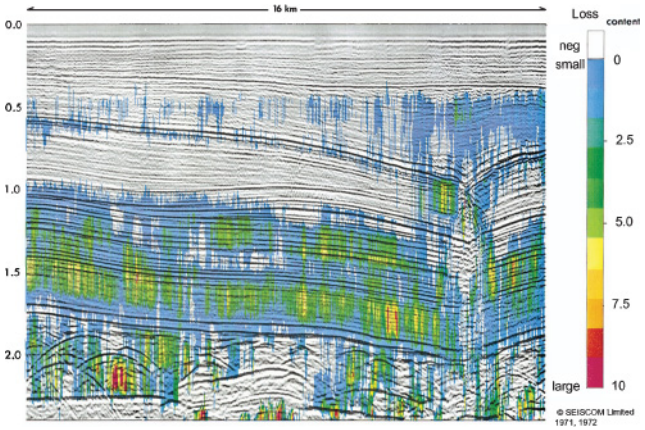

Figure 7. A composite attribute image from the early 1970s showing the differential frequency content (the relative loss of high frequencies down the section) superimposed on the structural section of Figure 3. (After Anstey, 2005.)

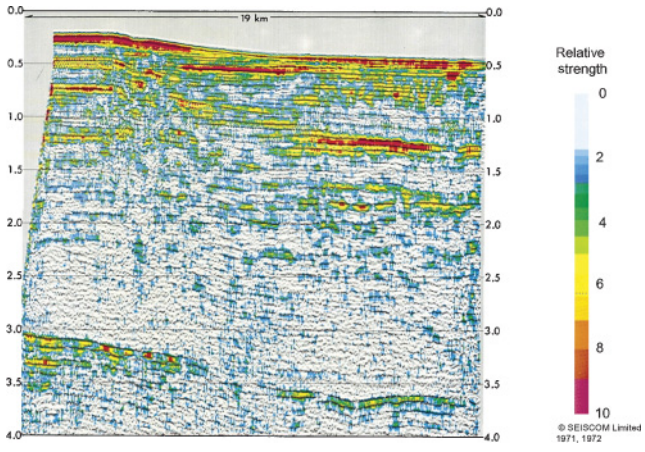

Figure 8. From the early 1970s, one of many bright spots identified in the North Sea. Display of reflection strength as in Figure 4. (After Anstey, 2005.)

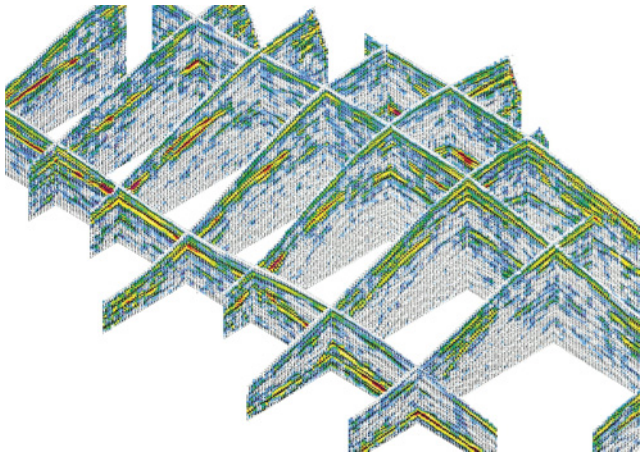

Figure 9. No substitute for 3D work, but valuable in its day. From the early 1970s, an isometric fence diagram of reflection strength on a grid of 2D lines over a gas field in the North Sea. (After Anstey, 2005.)

Norman Neidell, also working as a research geophysicist at Seiscom, came up with the suggestion that the Hilbert transform approach might be a useful way of achieving the same result. The Hilbert transform served as a starting point for the complex-trace analysis we now use routinely. Taner and Koehler continued this work and developed a single mathematical framework for attribute computation. The seismic trace amplitude is treated as the real part of the (complex) analytical signal while the imaginary part of the signal is computed by taking its Hilbert transform (Figure 10). The envelope is computed by taking the square root of the sum of the squares of the real and imaginary components, whereas the phase is computed by taking the double argument (ATAN2) inverse tangent of the imaginary and real components. Finally, the frequency is computed as the rate of change of the phase. These computations were carried out at each sample of the seismic trace and have since been dubbed instantaneous attributes. By 1975, three principal attributes — envelope, phase and frequency — were established:

1) Instantaneous envelope (reflection strength) is sensitive to changes in acoustic impedance and thus to lithology, porosity, hydrocarbons, and thin-bed tuning.
2) Instantaneous phase is useful for tracking reflector continuity and, therefore, for detecting unconformities, faults and lateral changes in stratigraphy.
3) Instantaneous frequency is useful in identifying abnormal attenuation and thin-bed tuning.

Seismic stratigraphy and complex-trace analysis

Taner presented his complex-trace analysis at the 1976 SEG meeting The timing for the development of this work proved to be opportune. Exploration activity was in full swing, driven by the energy crisis of the 1970s, while the principles of seismic stratigraphy were being introduced by Peter Vail and his colleagues at Exxon (Figure 11). As Taner remembers, "One day, as I displayed the instantaneous phase for a seismic profile, I was amazed to see the many different depositional patterns. I immediately called Peter and showed him the results I had.

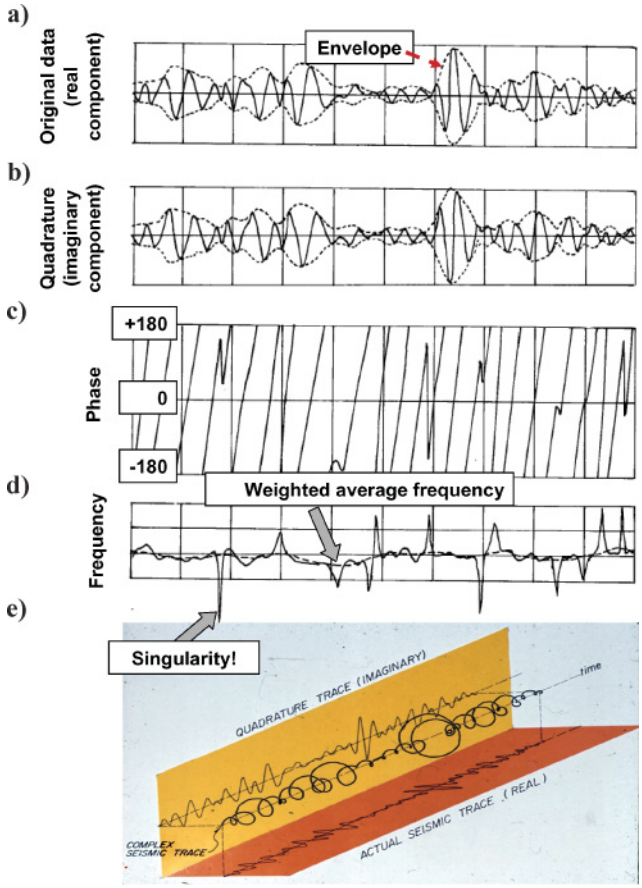

Figure 10. The (a) real seismic trace, (b) quadrature, (c) instantaneous phase, and (d) instantaneous frequency from Taner et al. (1979). Note the envelope-weighted frequency indicated by the dashed line in (d). Also note the singularities seen in instantaneous frequency due to waveform interference. (e) A scanned copy of a slide used by Tury Taner in presentations made during the 1970s to explain complex-trace analysis.

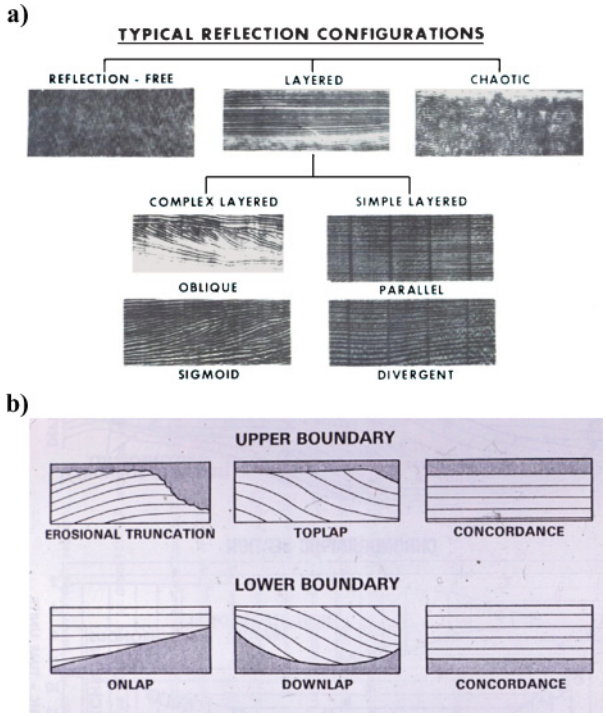

Figure 11. Scanned copies of two slides used by Tury Taner in the 1970s to illustrate the value of complex trace analysis applied to (a) a hard-streak lime buildup and (b) a gas-charged reservoir. Note the differences in polarity.

He was very impressed and said, 'That's the kind of section I would like to have for stratigraphic interpretation.' (T. Taner, personal communication, 2005).

Bob Sheriff (personal communication, 2005) recalls the 1976 AAPG meeting in Dallas where many of these advances were presented: "The presentations on seismic stratigraphy at the convention made such an impact that there was a request that the entire meeting be re-presented for those who had missed it. Instead, it was decided that a week-long seismic stratigraphy school would be more effective. This was only the 2nd school ever, and the AAPG continuing education coordinator was most effective in finding delightful off-season venues at delightful resorts around the country and internationally. This school was conducted for 7–8 years, with AAPG Memoir 26 (Payton, 1977) serving as the textbook."

While Vail et al. (1977) showed that seismic stratigraphy could be used as a measure of depositional processes, seismic attributes gained in popularity and respect. Taner, along with his colleagues Fulton Koehler and Bob Sheriff (who at the time was a member of the research team), published this work in two seminal papers (Taner and Sheriff, 1977; Taner et al., 1979) that helped geophysicists gain a better understanding of complex-trace analysis and its applications. In Figure 12. we display some of Taner's early displays of complex-attribute analysis of different lithologies.

Color plotting of seismic data

Alongside the theoretical evolution of complex-trace analysis, the hardware and software needed to do efficient color plotting were also developing during this time. Thus, by the late 1970s, color plotters had invaded the market and, as a result, time was right for the application of complex-trace analysis to aid seismic interpretation. Color plotting is thus an important piece of history, as the theoretical development would have had much less impact had there been no good way to display attributes in color.

Jamie Robertson (personal communication, 2005) recalls that seismic stratigraphy was an application that picked up and justified the expense of color plotting at Arco. Seismic stratigraphers saw the new color displays as tools to help pick event terminations, unconformities, and other fundamental inputs of seismic stratigraphy. In many oil companies, part of the justification for buying expensive plotters at the time was to plot seismic attribute sections and seismic stratigraphic analysis. In other companies, the expense was justified by the advent of 3D seismic data and the ability to display horizontal slices.

Seismic impedance inversion

During the mid-1970s, another significant seismic attribute contribution was inversion of poststack seismic amplitudes

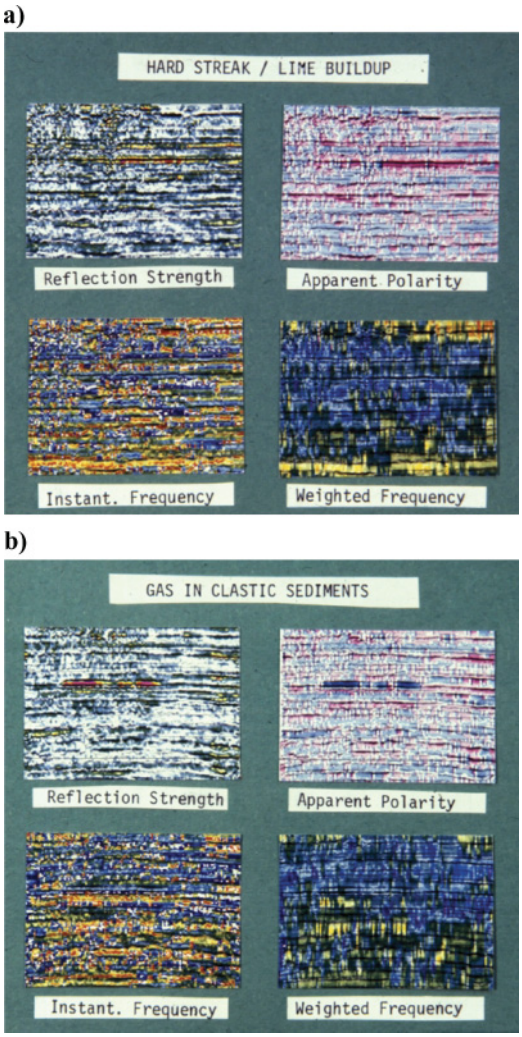

Figure 12. Scanned copies of two slides used by Tury Taner in the mid-1970s–1980s in the AAPG-sponsored school on seismic stratigraphy. (a) Representative reflection characters seen on 2D seismic lines. (b) Idealized characters used in seismic stratigraphy interpretation. These early interpretation workflows concepts provided the motivation for later developments in geometric attributes (including volumetric dip and azimuth, reflector parallelism, continuity, and unconformity indicators).

into acoustic impedance, an important physical property of rocks and an aid in studying the subsurface. The inverted impedance sections yielded useful information about the lateral changes in lithology and porosity. The conversion of seismic traces into acoustic impedance and velocity pseudo logs was first reported by Lavergne (1975) and Lindseth (1976, 1979), and they quickly became popular, mainly because of the ease and accuracy of interpretation of impedance data and also the stratigraphic interpretation framework that picked up at that time. Figure 13 shows an inverted seismic section from the Swan Hills Devonian reef bank that Lindseth used for prediction of carbonate porosity. At that time Lindseth used a transit-time scale rather than a velocity scale, and he also used a lithological color scale to highlight the changes in transit-time, which distinguished carbonate from clastic sections on the inverted acoustic impedance sections.

Seismic inversion for acoustic impedance is routinely used today. We include acoustic impedance with other attributes to be calibrated with well log data. Because of its early use of color overlays, impedance inversion was thought by many (especially company management that didn't want to pay for expensive plotters) to be no more than pretty colored wiggle traces. Indeed, 20 years later, Rebecca Latimer still felt it important to correct this misconception (Latimer et al., 2000).

Some shortcomings

A significant reality of the 1970s in many companies was that seismic data were interpreted by geophysicists rather than by geologists. The geophysicists engaged in processing at the time did a good job with structural imaging, arriving at noise-free, continuous reflections on the final processed sections. Unless schooled in the concepts of seismic stratigraphy, subtle discontinuities and fine detail associated with what we now interpret as slumps, turbidites, and other chaotic features could be lost. In general, the resolution of the seismic data in the 1970s was poor. Since few geologists were trained as geophysicists (Ravenne, 2002), the geophysical input to interpretation was missing, resulting in an erroneous product. There was often disagreement on the final results, with geologists arguing over geological input and geophysicists arguing about the uncertainty associated with interpretations based on reflections following a complex path as they travel in the subsurface. Thus, by the end of the 1970s, even though the concepts of seismic stratigraphy were developing, there were few well-established workflows — it was simply too difficult to estimate key lithologic parameters directly from trace data (May and May, 1991).

1980–1990

Incremental improvements

The 1980s saw a proliferation of seismic attributes with development of the cosine of instantaneous phase, dominant frequency, average amplitude, zero-crossing frequency, and many others. The cosine of instantaneous phase was developed, since it is a continuous parameter, unlike the phase itself, which has a discontinuity at $\pm 180^{\circ}$. Such a continuous attribute could be interpolated, smoothed, processed, and even migrated. The 1980s also saw the introduction of interval and formation attributes which measure an average property in a user-defined window centered about a picked horizon or, alternatively, between two picked horizons. Such windowed attributes are frequently used when the seismic reflections associated with a reservoir are sufficiently heterogeneous to preclude tracking a consistent peak or trough on all traces. These windowed attributes provide interval and formation attributes that are often more statistically meaningful than the instantaneous attributes, just as in well-log correlations, where we combine a number of thin, discontinuous sand units to generate a net-to-gross sand ratio map rather than maps specifying individual unit thicknesses.

A noteworthy observation was made by Robertson and Nogami (1984) — that the instantaneous frequency at the peak of a zero-phase seismic wavelet is equal to the average frequency of the wavelet's amplitude spectrum. That is to say,

there are points on a conventional instantaneous-frequency trace where the instantaneous frequency directly measures a property of the Fourier spectrum of the wavelet. For the same reason, the instantaneous phase corresponds to the wavelet's true phase at these points. These physically meaningful measurements occur at a small number of points. The remaining instantaneous-attribute measures provide little additional information about the seismic wavelet. Interpreters were frustrated when they attempted to do so to quantify reservoir properties. Later on, White (1991) showed that Robertson and Nogami's (1984) relationship between instantaneous frequency at the reflector peak and average spectrum does not statistically hold in practice because of noise and waveform interference.

Response attributes

The most stable of the instantaneous attributes was the envelope, which could always be counted on to provided accurate interval thicknesses. Bodine (1984, 1986) examined the instantaneous frequency and phase in terms of the reflection event estimated at the peak of the instantaneous envelope. He argued that since most of the signal energy in a trace is found in the vicinity of envelope peaks, the reflection event's phase and frequency could be more accurately described by assigning them to the value seen at peaks. While Bodine called these response attributes, we prefer Taner's more descriptive term of wavelet attributes. Thus, response (or wavelet) phase is the instantaneous phase at the point at which the envelope is maximum. One value is computed for each maximum and is applied to the width of the energy lobe from trough to trough. This phase is independent of the envelope and measures phase variations, one energy lobe to the next. Similarly, response frequency is the value of instantaneous frequency at the point at which the envelope is maximum and this single value is assigned to the width of the energy lobe between two successive troughs. Since the response frequency is calculated at envelope peaks, it avoids the singularities in the instantaneous phase (origin of the instantaneous frequency) seen where seismic events interfere, which is worst at the envelope troughs. [Hardage et al. (1998) later advocated using these discontinuities in instantaneous frequency for interpretation, while Taner (2001) developed a thin-bed indicator based on the difference between the singularity-resistive instantaneous frequency and the more smoothly varying envelope-weighted instantaneous frequency. These singularities will also form the basis of Liner et al.'s (2004) SPICE attribute.] These peak values were also the ones mapped later by Bahorich and Bridges (1992) in their seismic-sequence attribute mapping effort. Additional discussion of response attributes can be found in Robertson and Fisher (1988).

Early texture analyis

Inspired by the Sangree and Widmier's (1976) suggestion that zones of common seismic-signal character are related to the common geologic environment in which their constituent sediments were deposited, Love and Simaan (1984) attempted to extract these patterns using texture analysis. If a given signal character can be represented in the form of a 2D amplitude template, then it would be possible to classify every pixel by matching its local texture with the template of each feature. Further improvements to this template-matching process were made by incorporating artificial intelligence into the classification process. While such efforts were supposed to help with automatic analysis of large amounts of 2D surface-seismic data in a regionally consistent manner, they had very limited success, partly because of the low S/N ratio of the data and out-of-the-plane artifacts on 2D data. However, we conclude the biggest handicap was that 2D stratigraphic patterns could not be standardized. Twenty years later, with 3D data now routine, we realize the main problem was caused by the limitations of 2D seismic stratigraphy. Seismic patterns classified alternatively as "parallel," "sigmoidal," or "hummocky clinoforms" could all describe the same fan system — with the appearance depending on the orientation of the 2D acquisition over the fan, not on the geology.

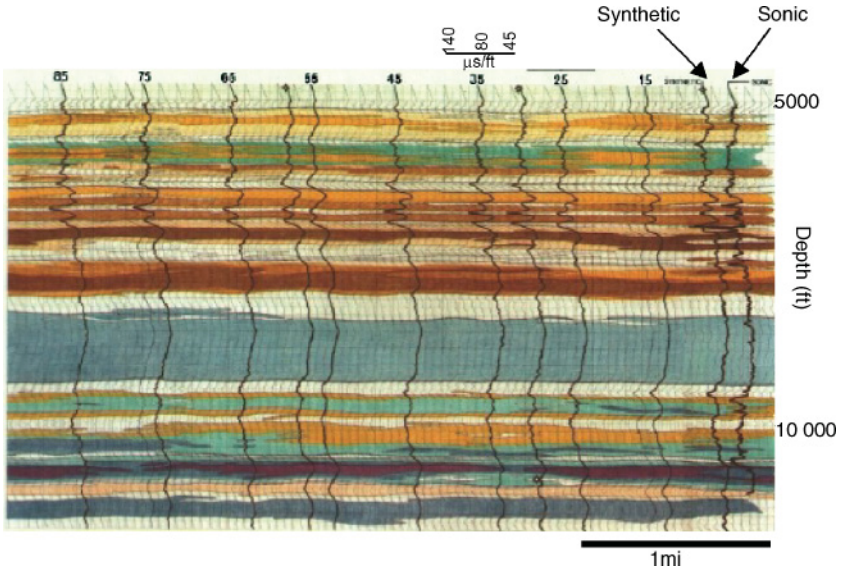

Figure 13. A Seislog inverted seismic section from the Swan Hills carbonate formation. (After Lindseth, 1979.)

Interpretive workstations

Development of interpretive workstations started in the 1980s in each of the major oil companies, first on mainframes, then on dedicated minicomputers, then on PCs, and finally on UNIX workstations. Hardware costs, initially high, plummeted rapidly. The second author remembers paying $120,000 for a dedicated PC system (that was less powerful than his current cell phone!). More interestingly, the dedicated workstation table (with three translational and two rotational degrees of freedom) cost $110,000! The 1980s saw a major shakeout in the interpretive workstation arena. The ever-increasing spiral of new computer standards burned out the not-so-nimble beginning-to-age geophysicists. Old software standards, such as the multiuser Uniras justified by the second author in the 1980s for $2,000,000 at Amoco, had too many legacy applications to keep up with the evolving

hardware. Most companies gave up internal development, and when the price of oil plummeted in the later half of the decade, outsourced workstation development and maintenance to vendors such as Scitex, Landmark, and Geoquest.

There were two main benefits of the interpretive workstation that beneficially influenced attributes. First, the use of color became pervasive and (unless you wanted a hard copy!) economical. Second, the calculation of a great many attributes became interactive. The benefit here was more one of personal risk reduction rather than speed. The daring interpreter could simply try out an idea in the dead of night and show favorable results to his or her boss the next day if it enhanced the map. If it failed, it was just one more computer file to be erased. There was no paper trail and, more importantly, no internal plotting cost, and no external contractor costs to explain to management. However, the ease of generating such attributes also leads to what Bob Sheriff calls "mindless interpretation."

There was one major disadvantage of this shakeout of oil company workstation development. The diversity of more than 20 research groups following their intuition and local business drivers in oil company laboratories were replaced by three or four software groups driven by customer demands and marketing constraints. Many good ideas were put in a "job jar" and died during this shakeout. We show one of these ideas in Figure 14, which is patterned after a presentation made by Knobloch (1982) while working on interpretation workstation software and workflows at Conoco. In it, we show an image of seismic data, instantaneous envelope, instantaneous phase, and a composite of instantaneous phase and envelope using a 2D color bar. Twenty-five years later, such a 2D color bar is still not provided by the three main workstation vendors (Scitex, Landmark, and Geoquest).

More colors and shaded relief maps

The number of colors expanded rapidly in the 1980s. The second author remembers many arguments about whether 8 or 16 colors were sufficient to display the information content of seismic data, primarily phase, frequency, envelope, and velocity. Those who were older (company management!) and conservative dressers (also management!) felt that 8 colors were sufficient. Interpreters favored 16. To analyze the sensitivity of the human eye, Knobloch (1982) displayed an image of Cheryl Tiegs (the cover girl of the era) in 2048 colors. Everyone agreed that Cheryl was a beautiful woman. He then dropped the display to 1024 colors. The 5% of the audience that were women all smiled — Cheryl had become pasty looking. By 512 colors the men noticed too, with poor Cheryl suffering from a bad case of acne. Knobloch's point was that of pattern recognition: the interpreter can see a great amount of detail through the use of colors if he or she has the experience or training.

Because of computer memory and input/output constraints, most of the commercial workstations settled on an 8-bit color display. Typically, five of these bits were used for color display of the seismic data (giving 32 colors), while the remaining three bits (8 colors) were used to display the interpretation. In this manner, an interpreter could toggle horizon and fault picks on and off by simply changing the color lookup table. While 24-bit color became widely available with UNIX-based workstations in the late 1980s, the cost of updating legacy applications forced most vendors until quite recently to continue to provide only 32 or 64 colors to the user. With the market push after 2000 to rewrite these legacy software applications for use on Linux and PC systems, these vendors now provide 256 colors.

The 1980s also saw the adoption of shaded relief maps (Batson et al., 1975), which became widely dispersed through the application to geophysical (SEASAT) measurements by Bill Haxby working at Lamont-Doherty Earth Observatory of Columbia University. Shaded relief maps of seismic data, including draped shaded relief maps with a 3D perspective, are now part of nearly all 3D seismic interpretation and visualization packages.

Autotrackers

Fortunately for practitioners, a few companies soldiered on with internal research and development. One of note is the work initiated by Naaman Keskes at the French National Robotics and Computer Lab (INRIA), supported in part by Elf Aquitaine. Keskes and his colleagues used a suite of attributes, including instantaneous dip, semblance, amplitude, phase, and frequency to track "seeded" picks around a grid of 2D seismic lines. Keskes later joined Elf Aquitaine in Pau,

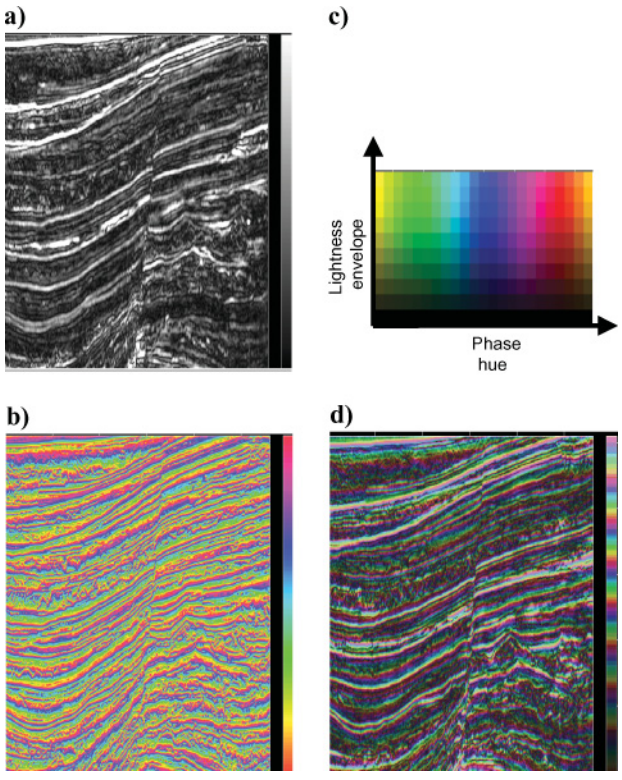

Figure 14. Combining (a) reflection envelope and (b) reflection phase using (c) a 2D color bar to form (d) a composite image. This technique, originally presented by Knobloch (1982), emphasizes the phase of the stronger reflection events and provides an effective tool for tracking waveforms across faults. The 2D color legend (c) has been mapped to a more conventional 1D color legend in (d) in order to use conventional plotting software.

where he was one of the key designers of their internal Sismage product (Keskes et al., 1982, 1983; Sibille et al., 1984). A derivative of Sismage, commercialized 15 years later under the name Stratimagic, is now one of the more popular attribute-analysis applications.

As a side note, a contemporary in the French university system, Evgeny Landa, was also sponsored by Elf Aquitaine. While Elf's focus was velocity analysis for prestack depth migration (Landa et al., 1989), its tools consisted of complex traces, semblance, and dip attributes. Scheuer and Oldenburg (1988) also used complex-trace analysis for velocity analysis. Their work formed the basis for 2D (and later 3D) dip and azimuth computation by Barnes (1996), who at that time was collaborating with Taner. Taner (2001) also addressed the autotracking problem, but with an emphasis on first break picking for refraction statics. In short, attributes technology was used and enhanced by processing needs and developments.

In summary, the 1980s saw a rapid expansion in the seismic processing and display capabilities necessary for the explosion of attribute techniques that would occur in the mid-1990s. However, attribute usage in the 1980s actually decreased in comparison to the late 1970s.

Attributes fall out of favor

Complex-trace attributes suffer from waveform interference arising from nearby interfaces that can obscure subtle trends in the data. In particular, instantaneous-frequency estimates can fall outside the seismic bandwidth and even generate negative values. Although a few workers understood this phenomenon and could use it as an unconformity or thin-bed indicator, the deleterious consequences of waveform interference was not published, so interpreters attempting to associate physical meaning with such attributes were frustrated by such artifacts. They also found it difficult to relate these attributes directly to logged reservoir properties such as porosity; thus, they could not be used to quantify reservoir properties. As the 1980s passed, seismic attributes lost credibility with interpreters. This loss was probably coupled with a loss of faith in seismic stratigraphy as well, as numerous dry holes were drilled based on seismic stratigraphic predictions. Jamie Robertson (personal communication, 2005) lists some the contributing factors as follows.

1) Given the limited resolution of the seismic data available in the 1980s, coupled with the lack of geological input to interpretation, interpreters lost sight of what seismic data could really resolve compared to the stratigraphic resolution they were seeking. Numerous interpretations of geological detail simply were unjustified by the resolution of the seismic data. When geologists attempted interpretations of seismic attributes, they often did not have a sound understanding of the limitations of seismic data, and their geophysicist teammates did not do a good job of educating them in the pitfalls of the seismic resolution.
2) Three-dimensional seismic surveying began in the early 1970s and by the mid-1980s emerged as a beneficial technique in many onshore and offshore areas around the world. It improved resolution enormously and contributed effectively fewer dry wells. Even though it was considered expensive at the time, 3D seismic interpretation proved to be much better at making successful exploration predictions than seismic stratigraphic analysis of 2D seismic data. This had a dampening effect on the use of 2D seismic stratigraphic interpretation of attribute sections. Use of attribute techniques only reemerged after workstation tools were developed to apply the technology to 3D data.
3) After the energy crisis of the 1970s and the accompanying oil-price rise, oil companies in the early 1980s scrambled to drill prospects and were not careful to drill only the good ones. Exploration management, in essence, allowed too many poor prospects to be drilled, and seismic stratigraphy/attribute analysis took the blame for failure when the blame really should have gone to poor exploration management judgment or overly optimistic predictions about the price of oil.

Other experts at the time also voiced their concerns about this state in which seismic attributes were found, and Barnes (2001) gives excerpts from the literature.

Seismic stratigraphy faced an additional problem with 3D data. One of the more common workflows on 2D data was to generate "A – B over C" interpretations on seismic sections and then post symbols for "parallel," "hummocky," "chaotic," and so forth manually on maps, which were then contoured. Three-dimensional data precluded posting such dense alphanumeric information. It was not uncommon for the stratigrapher member of the team to extract several key 2D lines and go off to do hard-copy interpretation while the rest of the team was deeply immersed in the digital world.

We should note that while complex-trace attributes of seismic traces revealed aspects that otherwise often went unnoticed, these complex-trace attributes did not create any new information. While complex-attribute analysis produces additional sections which tend to point out certain aspects of geology that were masked on the variable-area/wiggle-trace seismic sections, a skilled interpreter with sufficient time could extract all the necessary details using conventional interpretation techniques. Seismic-sequence attribute mapping (simply stated, the mapping of extracted attributes much like picked traveltimes) developed by Bahorich and Bridges (1992) would allow us to extract attributes from 2D data and generate an attribute map. Time slices, horizon slices, and arbitrary vertical traverses through attribute volumes generated for 3D data would provide such images directly.

We should also recall that seismic data was expensive to collect and process during this time. Fifty percent of geophysicists were involved in acquisition and processing, with the remainder making maps (interpretation). Today, 15–20 years later, while the vast majority of geophysicists are interpreters, data volumes have increased so rapidly that most seismic lines may never be individually inspected or manually picked.

Two-dimensional attributes

By the mid-1980s, considerable improvements in recording and processing techniques had enhanced the information content of seismic data required for stratigraphic interpretation. During this time, a number of 2D continuity and dip attributes were developed that were employed in procedures for defining and analyzing seismic facies (Conticini, 1984; Vossler, 1988). Finn (1986) anticipated the need for 3D estimates of dip

and azimuth by applying a 2D semblance estimate of apparent dip on surveys of 2D intersecting lines. Though novel and interesting, these procedures did not evoke an enthusiastic response. The results could be subjective, and 2D surveys simply contained too many artifacts from out-of-plane reflections.

Horizon/interval attributes

Toward the middle of the 1980s and later, horizon attributes (Dalley et al., 1989) and interval attributes (Sonneland et al., 1989) were introduced that demonstrated that interpreted horizons exhibited reflector characteristics not easily observed on the vertical seismic sections. The areal variation in reflection characteristics could be related to paleogeographic elements (Brown and Robertson, 1985), while the amplitude extractions of seismic horizons revealed features directly related to stratigraphic events. These amplitude extraction maps were used to interpolate/extrapolate reservoir properties from well control (Thadani et al., 1987). The most important of the references establishing these work flows is Alistair Brown's (1986) AAPG Memoir 42.

1990–2005

Industry adoption of 3D seismic

The 1990s brought new life to seismic attribute analysis. The industry had by now embraced 3D technology, by far the most successful new exploration technology of several decades. By its very nature, 3D required computer-aided interpretation which led to optimized well locations that were presented to the drilling decision teams. Perhaps the single most important contribution in making these drilling decisions at this time was the concept of 3D attribute extractions. One of the earliest 3D attribute publications is by Dalley et al. (1989) and his colleagues at Shell. Rijks and Jauffred (1991) introduced two concepts that are now commonplace in the interpretation workplace: dip/azimuth maps and amplitude extractions. In Figure 15, we reproduce a suite of images from Rijks and Jauffred (1991), including a vertical section through the seismic data showing the picked top and bottom of the formation in Figure 15a, a dip magnitude map of the upper horizon in Figure 15b, a shaded relief map of the same horizon in Figure 15c, and amplitude extractions from both the upper and lower horizons in Figure 15d and e. These images not only showed the value of 3D seismic data, they also established standard workflows that are still accepted as best practices today.

The association of attributes with 3D seismic breathed new life into attribute analysis, moving it away from seismic stratigraphy and toward exploitation and reservoir characterization. Contemporaneous developments in rock physics research provided the quantitative basis of how rock properties affect seismic data, allowing us today to directly relate attributes to rock properties in a much more credible way than was possible in the 1980s (Jaime Robertson, personal communication, 2005).

Seismic-sequence attribute mapping

It is counterintuitive that making maps of attributes generated on 2D surveys did not occur until similar maps were made directly from 3D data. While complex-trace analysis numerically quantified subtle changes in envelope, amplitude, and phase, these same attributes of the data could be readily seen by an experienced interpreter from the original

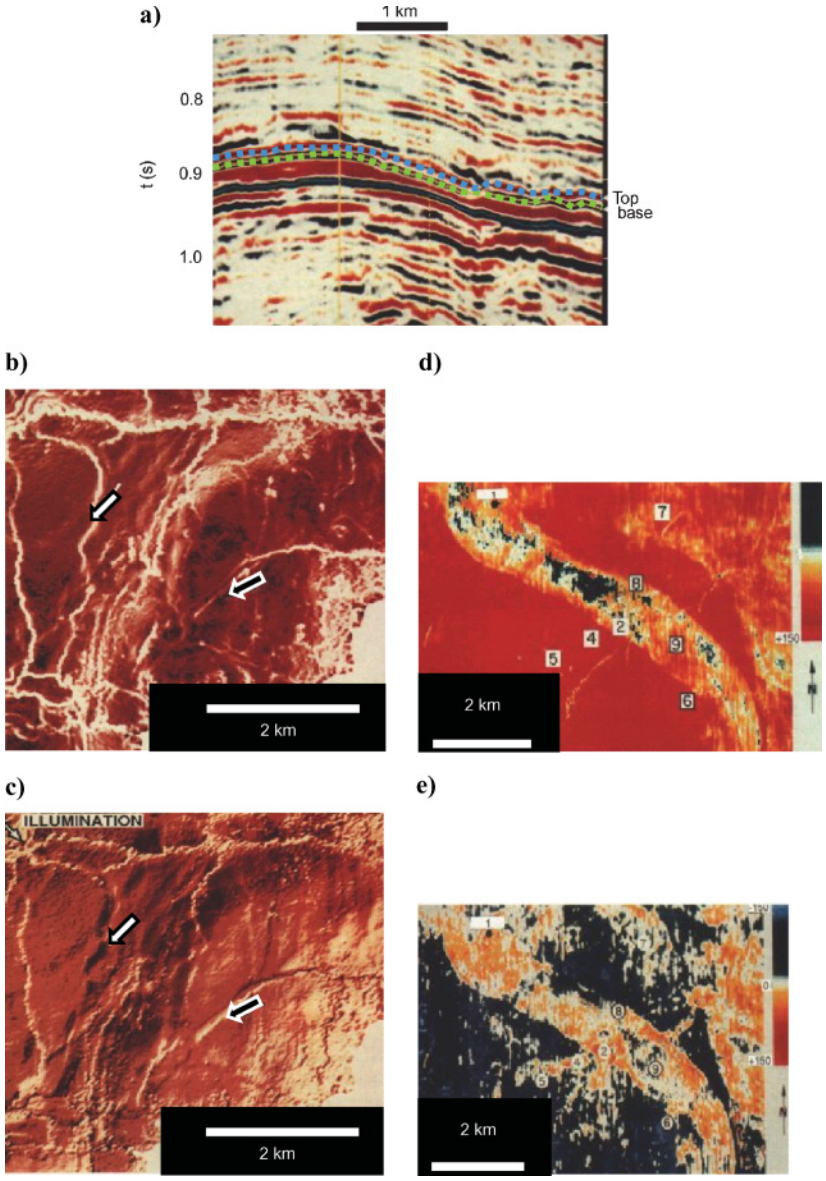

Figure 15. (a) A vertical section through a 3D seismic data volume with a picked top (blue dots) and bottom (green dots) of a formation. (b) A dip magnitude and (c) a shaded relief map of the top reflector. Amplitude extractions (a "horizon slice" through the seismic data) corresponding to the (d) bottom and (e) top reflector. The white arrow indicates a small 10-m throw graben confirmed by seismic data that is seen in the shaded relief map. (After Rijks and Jauffred, 1991.)

seismic data itself. However, such human interpretation could not readily be turned into a map. The key steps were first presented by Sonneland et al. (1989), followed by Bahorich and Bridges (1992) and Bahorich and van Bemmel (1992), who presented this concept as the seismic-sequence attribute map (SSAM). Interestingly, Amoco's involvement in this effort took place out of its Denver exploration office rather than its research center in Tulsa. Having unwillingly given up internal workstation development in the late 1980s, Amoco's research efforts (like most other companies) were focused on "more important" technologies, including prestack depth migration and AVO. Bahorich (then at the Denver office) proselytized the value of SSAM so strongly that eventually he was "punished" and sent to dwell with the technology misfits in Tulsa, thereby solving the "problems" of both groups. This fortuitous occurrence soon lead to Amoco's development of seismic coherence.

Three-dimensional seismic exploration comes of age

By the mid-1990s, 3D seismic technology became affordable. Whereas by 1980, only 100 3D seismic surveys had been done, by the mid-1990s an estimated 200–300 3D surveys were being conducted annually. Good 3D interpretation workflows on interactive workstations were being perfected. Complex-trace analysis was performed on full 3D seismic volumes and used in the interpretations. However, most 3D interpretation was performed on vertical inlines and crosslines and then projected onto a time slice. Though this worked well, it led to ambiguities in the lateral placement of faults, especially where faults joined together, crossed, or simply ended as a result of changes in geologic stress.

Seismic coherence

Although 3D was routinely used for exploitation, Amoco still primarily used 2D for exploration in the early 1990s. Bahorich, now imprisoned with (and accused of being one of!) Amoco's researchers, was faced with the problem of making his seismic-sequence attribute-mapping workflow produce useful results in multiple overlapping 2D surveys. Since the data had radically different amplitude, phase, and frequency, there was little that could be done in an interpretative workstation; phase and spectral matching required reprocessing. Instead, working with programmer Steve Farmer, Bahorich evaluated several alternative attributes that were relatively insensitive to the source wavelet. By computing and mapping a normalized crosscorrelation between adjacent traces in the same survey, the variability of source-wavelet amplitude and phase could be eliminated, and waveform continuity could be quantified. [Unbeknownst to the Amoco team, this was Finn's (1986) M.S. thesis, though Finn did not have a ready means of posting his data in map view.] Faults were easily seen and could be tracked on the 2D section. Within a week of this development, John Lopez, a structural geologist member of the team working out of Amoco's New Orleans office, applied it to a large 3D data set. The results were astounding. Seismic coherence was born. Although the idea of coherence was conceptualized earlier in different ways by different researchers (Drecun and Lucas, 1985; Claerbout, 1990), the development and application of coherence to 3D seismic data, in the form of "coherence cube" technology, took the industry by storm.

Bahorich and Farmer (1995, 1053) state that their coherence methodology was the "first published method of revealing fault surfaces within a 3D volume for which no fault reflections had been recorded." Their volume of coherence coefficients computed from the seismic amplitudes on adjacent traces using a crosscorrelation technique, clearly portrayed faults and other stratigraphic anomalies on time and horizontal slices. The coherence images distinctly revealed buried deltas, river channels, reefs, and dewatering features. The remarkable detail with which stratigraphic features show up on coherence displays, with no interpretation bias and some previously unidentifiable even with close scrutiny, appealed to the interpreters. They had a new view of their data. The Amoco team followed their original three-trace crosscorrelation algorithm with semblance and eigendecomposition coherence estimates (Marfurt et al., 1998, 1999; Gersztenkorn and Marfurt, 1999), which provided improved clarity and lateral resolution (Chopra, 2002). According to SEG's citation recognizing this contribution, "this significantly changed the way geophysicists interpret 3D seismic data and the way oil industry management views geophysicists' contributions to the industry."

Figure 16 depicts an example from offshore East Coast of Canada, where northwest-southeast faults and fractures, apparently difficult to interpret, show up clearly on coherence time slices. Overlaying coherence on a seismic time slice provides the interpreter with the capability to more easily name and link master and antithetic faults.

Spectral decomposition

Another Amoco interpreter, this time from Calgary, cried out for attention from his research colleagues in Tulsa. Greg Partyka had generated some enticing images of poorly resolved reef plays in Canada using short-window Fourier transforms. The research supervisor in Tulsa (the second author of this article), felt that the spectral analysis problem was already well understood, given the previous work by Kallweit and Wood (1982) and Okaya (1995). Again, the proselytizer and the miscreant were soon cell mates in Tulsa and forced to live in harmony. Once in the research environment, Partyka partnered with the signal analysis team (James Gridley) and interpreters (John

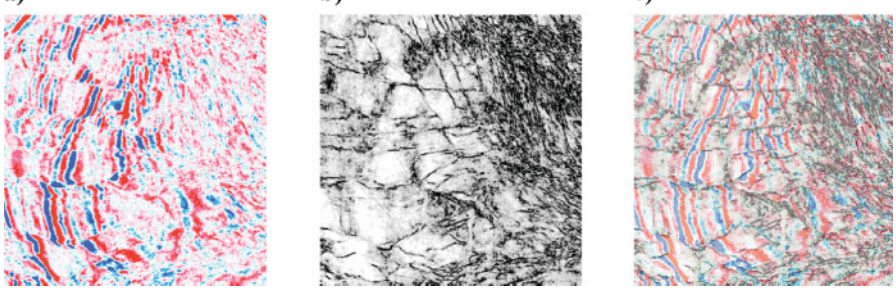

Figure 16. Time slices through (a) a seismic and (b) coherence data volumes. (c) Overlay of coherence on seismic. Note that the coherence slice not only reveals faults with clarity but also the intensively fractured region to the right. (After Chopra, 2002.)

Lopez in New Orleans and Lynn Peyton in Denver) and applied his technique to 3D data where, like many other attributes displayed in 3D map and horizon slices, it made a significant interpretational impact (Partyka et al., 1999; Peyton et al., 1998). Spectral decomposition was born. This work continues actively today, with most workers preferring the wavelet transform–based approach introduced by Castagna et al. (2003) over the original discrete Fourier transform.

Seismic inversion revisited

The original recursive or trace-integration seismic inversion technique for acoustic impedance also evolved during the late 1980s and 1990s, with developments in model-based inversion, sparse-spike inversion, stratigraphic inversion, and geostatistical inversion providing accurate results (Chopra and Kuhn, 2001). The earlier techniques used a local optimization method that produced good results when provided with an accurate starting model. Local optimization techniques were followed by global optimization methods that gave reasonable results even with sparse well control.

Connolly (1999) introduced elastic impedance, which computes conventional acoustic impedance for nonnormal angle of incidence. This was further enhanced by Whitcombe (2002) to reflect different elastic parameters such as Lamé's parameter λ, bulk modulus κ, and shear modulus μ.

Crossplotting of attributes

Crossplotting of attributes was introduced to visually display the relationship between two or three variables (White, 1991). Verm and Hilterman (1994) used crossplots in AVO analysis, which have been used since as AVO anomaly indicators. When appropriate pairs of attributes are crossplotted, common lithologies and fluid types often cluster together, providing a straightforward interpretation. The off-trend aggregations can then be more elaborately evaluated as potential hydrocarbon indicators, keeping in mind the fact that data that are anomalous statistically are geologically interesting — the essence of successful AVO-crossplot analysis. Extension of crossplots to three dimensions is beneficial, as data clusters hanging in 3D space are more readily diagnostic, resulting in more accurate and reliable interpretation.

In Figure 17, we illustrate the use of modern crossplotting software of three attributes that help identify a gas anomaly: λ-ρ on the x-axis, μ-ρ on the y-axis, and fluid stack on the z-axis. In Figure 17a, we indicate a gas anomaly on a time slice through the λ-ρ volume by a blue patch. We then draw a red polygon on the time slice (outline) to select live data points to be displayed in the crossplot. The red cluster of points in Figure 17b corresponds to the red polygon and five time slices (two above and two below the one shown). As the crossplot is rotated toward the left on the vertical axis, the fluid stack shows the expected negative values for the gas sand (Figure 17c). The yellow and magenta clusters in Figure 17b and c are the corresponding contributions from the yellow and red polygons in Figure 17a.

Automated pattern recognition on attributes

The attribute proliferation of the 1980s resulted in an explosion in the attribute alternatives available to geophysicists. Besides being overwhelming, the sheer volume of data defied attempts to gauge the information contained within those data using conventional analytical tools and made their meaningful and timely interpretation a challenge. For this reason, one school of geophysicists examined automated pattern-recognition techniques (de Figueiredo, 1982) wherein a computer is trained to determine the patterns of interest and sift through the available bulk of data seeking those patterns.

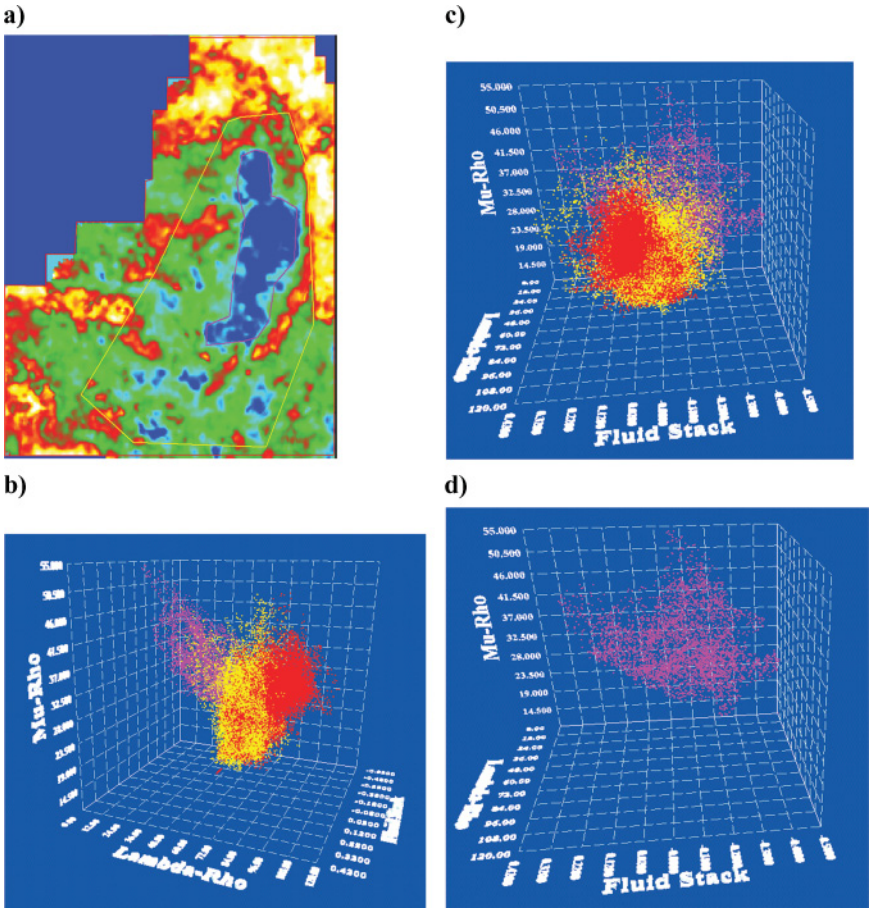

Figure 17. A λ-ρ section (with polygons selected) and corresponding clusters on 3D crossplots. (a) Polygons selected on a time slice from the λ-ρ volume. The red-bordered polygon indicates the area being analyzed. (b) Points within the red, yellow, and purple polygons show up as different clusters. The gas anomaly (blue on the time slice and enclosed by the purple polygon) shows up with negative values for the fluid stack. (c) 3D crossplot seen from the fluid-stack side. (d) 3D crossplot seen from the fluid-stack side and including only points from the purple polygon. (After Chopra et al., 2003.)

A second school of geophysicists began combining attributes sensitive to relevant geological features through multiattribute analysis.

Neural network application for multiattribute analysis

One attempt at automated pattern recognition took the form of neural networks (Russell et al., 1997), wherein a set of input patterns is related to the output by a transformation that is encoded in the network weights. In Figure 18, we show an example of how multivariate statistical analysis can be used in determining whether the derived property volumes are related to gas saturation and lithology (Chopra and Pruden, 2003). For the case study from southern Alberta, it was found that the gamma-ray logs in the area were diagnostic of sands, and there was a fairly even sampling of well data across the field. A nonlinear multiattribute-determinant analysis was employed between the derived multiple seismic-attribute volumes and the measured gamma-ray values at wells. By training a neural network with a statistically representative population of the targeted log responses (gamma ray, sonic, and bulk density) and the multiple seismic-attribute volumes available at each well, a nonlinear multiattribute transform was computed to produce gamma-ray and bulk-density inversions across the 3D seismic volume.

In Figure 18a and b, we show the λ-ρ and μ-ρ sections with the anomaly enclosed in yellow polygons. The crossplots for these two attributes are also shown (Figure 18c). The yellow dots on the crossplots represent the values within the polygons in Figure 18a and b. The magenta polygon in Figure 19c indicates where we would expect to find gas sands in λ-ρ and μ-ρ space in Figure 19a and b, respectively. The results of the gamma inversion are shown in Figure 20. The data are scaled to API gamma units in Figure 20a and converted to porosity in Figure 20b using the standard linear-density relationship. From log data, the sand-filled channels are interpreted as having gamma values less than 50 API units. This cutoff value was used to mask out inverted density values for silts and shales. Analysis of Figure 20a and b shows three distinct sand-bearing channels. Cubic B-spline curves (mathematical representation of the approximating curves in the form of polynomials) have also been used for determination of mathematical relationships between pairs of variables for well logs; those relationships were then used to invert attribute volumes into useful inversion volumes such as gamma ray and porosity (Chopra et al., 2004). In Figure 21, we show spline curve–inverted porosity.

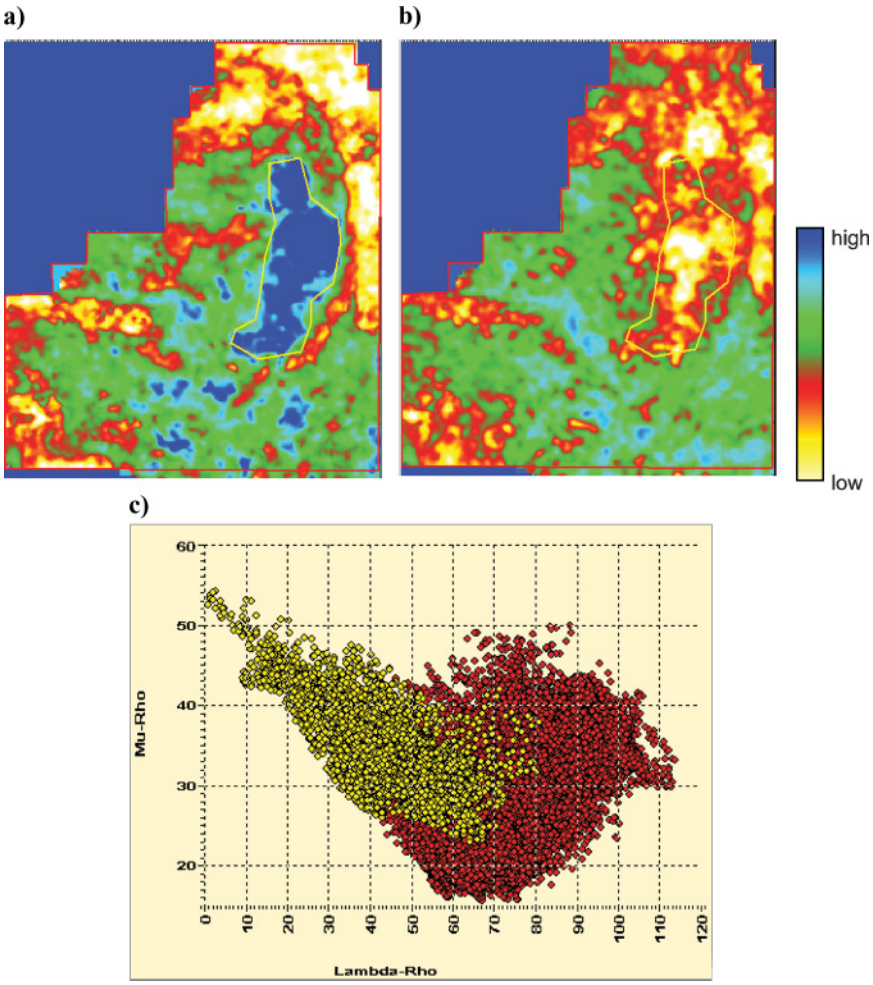

Figure 18. Time slices through (a) λ-ρ and (b) μ-ρ volumes. The suspected gas anomaly is indicated by low (blue) values in the λ-ρ slice and high (yellow) values of μ-ρ in the μ-ρ slice. (c) Crossplot of λ-ρ versus μ-ρ. The red polygon encloses all the live data points on both time slices, whereas the yellow polygon encloses the suspected anomaly. The crossplot shows the yellow points corresponding to low values of λ-ρ and high values of μ-ρ that is expected of a gas anomaly. (After Chopra and Pruden, 2003.)

Enhanced visualization helps attribute interpretation

Gradually, as geophysicists realized that the additional benefits provided by 3D seismics were beneficial for stratigraphic interpretation of data, seismic-interpretation methods also shifted from simple horizon-based to volume-based work. This provided interpreters new insights that were gained by studying objects of different geological origins and their spatial relationships. In Figure 22, we display strat cubes (subvolumes bounded by two not necessarily parallel horizons) generated from the seismic and the coherence volumes. The coherence strat cube indicates the north-south channel very clearly, the east-west fault on the right side, as well as the downthrown side of the north-south fault on the left.

Of course, with all this also came the complexity and the magnitude of identification work and the need for faster and more accurate tools. This brought about the significant introduction of techniques for automated identification of seismic

objects and stratigraphic features Keeping pace with such emerging technologies were advancements in visualization, all of which modernized the art of seismic interpretation. Starting at the seed voxels, a seed tracker will search for connected voxels that satisfy the user-defined search criteria, thereby generating a 3D "geobody" within the 3D seismic volume.

While one given attribute will be sensitive to a specific geologic feature of interest, a second attribute may be sensitive to a different kind of feature. We can therefore combine multiple attributes to enhance the contrast between features of interest and their surroundings. Different methodologies have been developed to recognize such features. Meldahl et al. (2001) used neural networks trained on combinations of attributes to recognize features that were first identified in a seed interpretation. The network transforms the chosen attributes into a new "meta attribute," which indicates the probability of occurrence of the identified feature at different seismic positions. Such highlighted features definitely benefit from the knowledge of shapes and orientations of the features that can be added to the process.

Trace shape

While spectral decomposition and wavelet analysis compare seismic waveform to precomputed waveforms (typically, windowed tapered sines and cosines), an important development was released by Elf Aquitaine in the mid-1990s: trace-shape classification. In this approach, the interpreter defines a zone of interest pegged to an interpreted horizon, then asks the computer to define a suite of approximately 10–20 waveforms (classes) that best express the data. The most useful of these classifiers is based on self-organized maps (Coleou et al., 2003) whose appearance is relatively insensitive to the number of classes. Although the results can be calibrated to well control through forward modeling, and although actual well classes can be inserted, this technology is particularly well suited to a geomorphology-driven interpretation, whereby the interpreter identifies depositional and structural patterns from the images and, from these, infers reservoir properties.

Texture attributes

More recently the idea of studying seismic textures has been revived. While the term was earlier applied to seismic sections to pick out zones of common signal character (Love and Simaan, 1984), studies are now underway to use statistical measures to classify textures using gray-level co-occurrence matrices (Vinther et al., 1995; Vinther, 1997; Whitehead et al., 1999; West et al., 2002; Gao, 2003, 2004). Some of the statistical measures used are energy (denoting textural homogeneity), entropy (measuring predictability from one texel or voxel to another), contrast (emphasizing the difference in amplitude of neighboring voxels), and homogeneity (highlighting the overall smoothness of the amplitude). Energy, contrast, and entropy have been found to be the most effective in characterizing seismic data.

Figure 23 shows a comparison of the amplitude and energy horizon slice at the same stratigraphic level. Notice that the channel/levee deposits can be recognized, mapped, and detected more effectively from the volume than from the amplitude volume. [Note: The original definition of energy as first given by Haralick et al. (1973) has been redefined as homogeneity by Gao (2003).]

Curvature

With the wide availability of 3D seismics and a renewed interest in fractures, we have seen a rapid acceleration in the use of curvature maps. The structural geology relationship between curvature and fractures is well established (Lisle, 1994) though the exact relationship between open fractures,

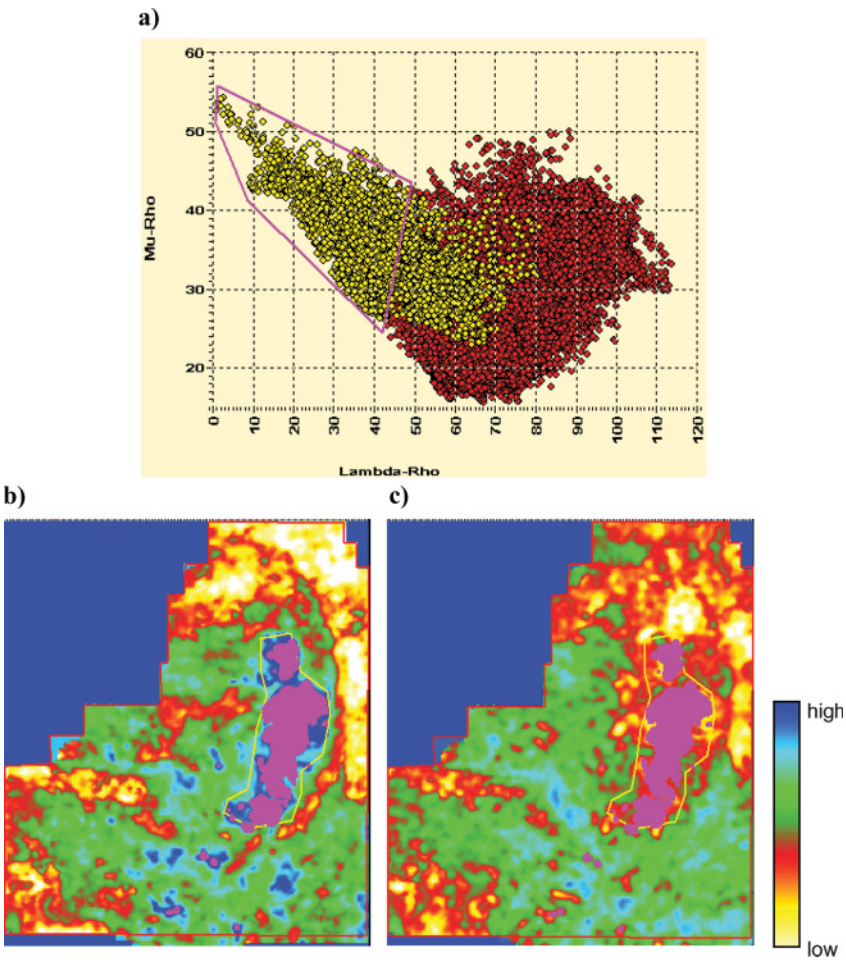

Figure 19. (a) Enclosing the low values of λ-μ and high values of μ-ρ in Figure 18c with the magenta polygon highlights their corresponding spatial locations on the (b) λ-ρ and (c) μ-ρ time slices. The job of the interpreter is then to validate his seismic attributes with his or her interpretation of the depositional and structural setting. (After Chopra and Pruden, 2003.)

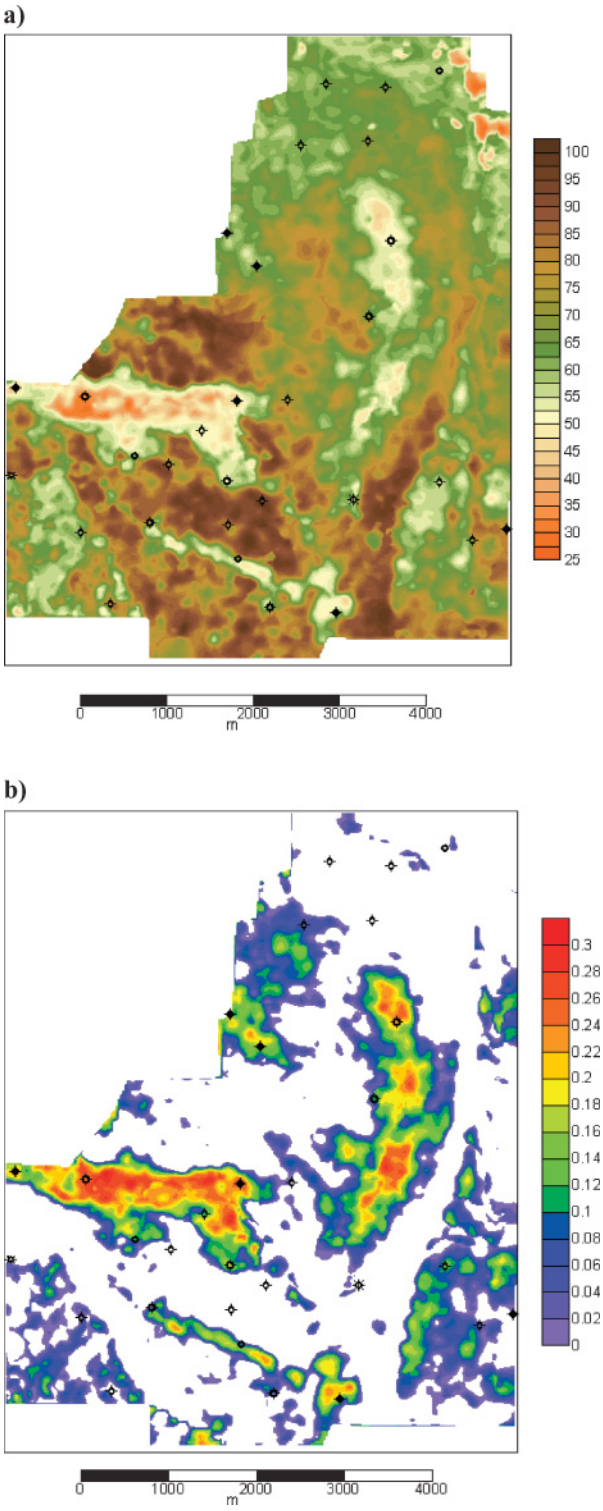

Figure 20. (a) Neural network–inverted gamma-ray response. Note the distinct separation of sand from silt and shale. (b) Neural network–computed porosity from the inverted density response. The density values have been masked out for gamma-ray values representative of silt or shale, giving a relative porosity indicator for the sands. (After Chopra and Pruden, 2003.)

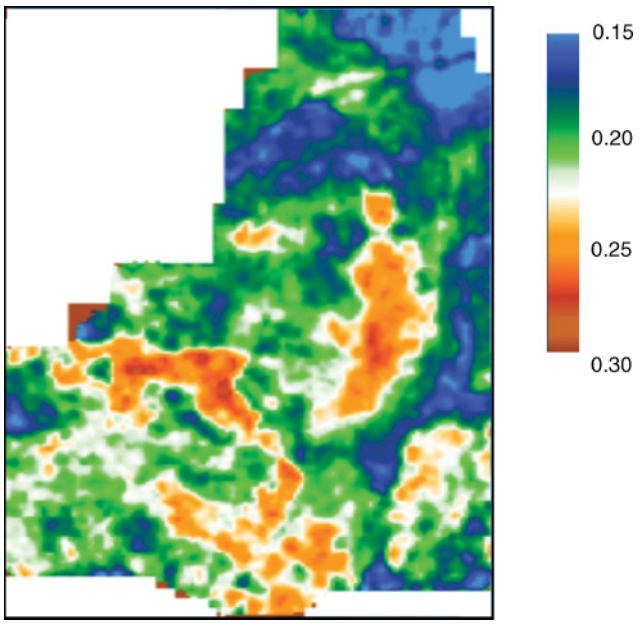

Figure 21. Spline curve–inverted porosity corresponding to the time slices shown in Figures 19 and 20. (After Chopra et al., 2004.)

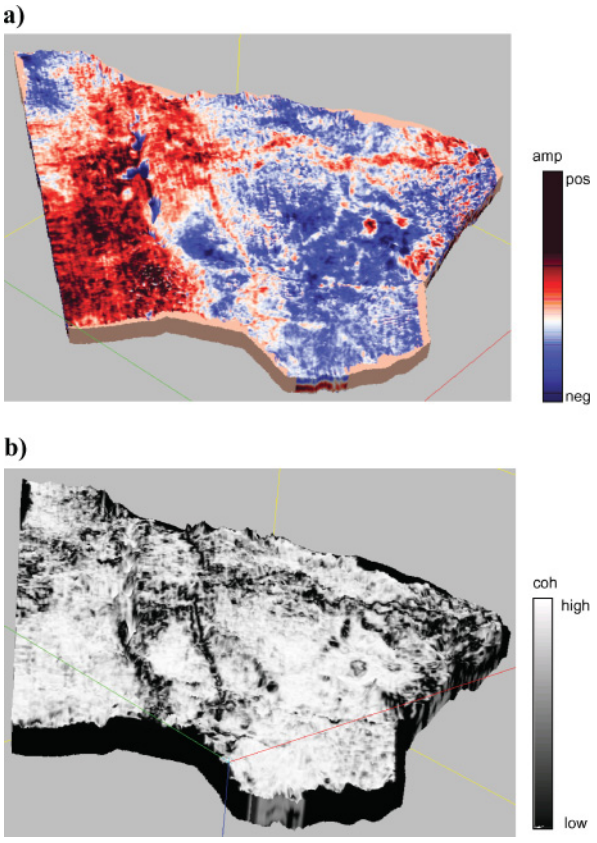

Figure 22. Strat cubes (a subvolume of 60-ms thickness bounded by two not necessarily parallel horizons) of the (a) seismic and (b) coherence volumes. Notice the clarity with which the north-south narrow channel is seen on the coherence strat cube and also the fault (seen with the help of relief). An east-west fault trend is also clearly seen on the coherence strat cube. (Data courtesy of Arcis Corporation, Calgary.)

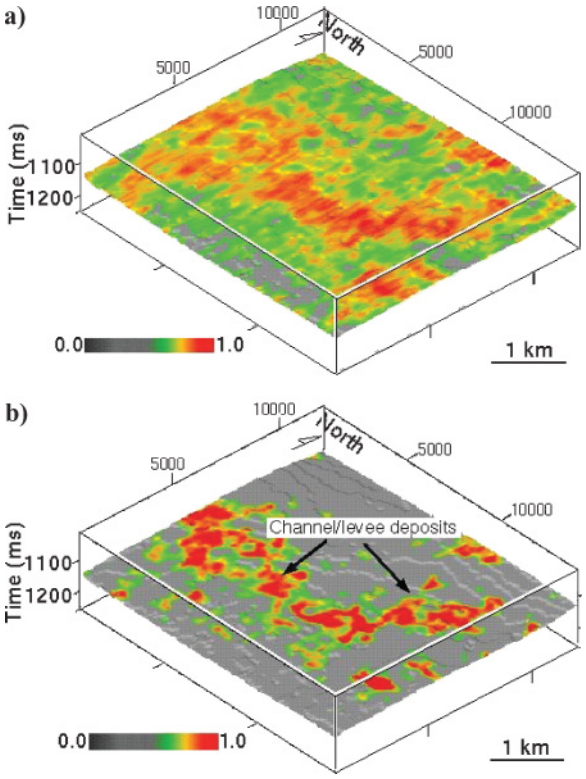

Figure 23. A comparison between average absolute amplitude (a) and energy (b) in a horizon slice at the same stratigraphic level. To avoid a biased comparison, the same processing parameters (texel size and dimension) and a normalized color-mapping function are used. Notice that the channel/levee deposits can be recognized, mapped, and detected more effectively from the energy volume than from the amplitude volume. (After Gao, 2003.)

paleostructure, and present-day stress is not yet clearly understood. Roberts (2001), Hart et al. (2002), Sigismondi and Soldo (2003), Masaferro et al. (2003), and others have used seismic measures of reflector curvature to map subtle features and predict fractures. Curvature (a 3D property of a quadratic surface that quantifies the degree to which the surface deviates from being planar) attribute analysis of surfaces helps to remove the effects of regional dip and emphasizes small-scale features that might be associated with primary depositional features or small-scale faults. Figure 24 shows minimum curvature draped over a near-basement reflection in part of the San Juan Basin. A prominent north-south-trending incised valley is apparent, as are some faults that strike approximately northwest-southeast.

Figure 25a shows a time-structure map of the top of a Tertiary incised channel-levee complex. Figure 25b and c shows the dip component of curvature overlain on a 3D representation of the horizon with shaded relief to enhance features. Note how by changing the viewing angle, zoom, and surface illumination angle, the definition of stratigraphic and structural features can be improved compared to the time-structure map.

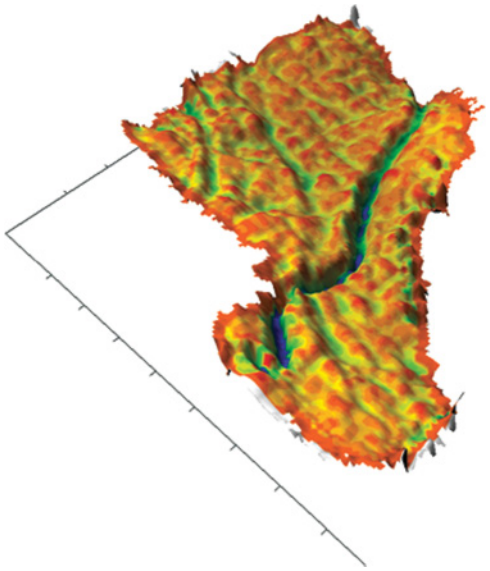

Figure 24. This image shows minimum curvature draped over a near-basement reflection in part of the San Juan Basin. A prominent north-south-trending incised valley is apparent, as are some curvilinear faults that strike approximately northwest-southeast. Tick marks are 1 km. Illumination from the southwest. (Image courtesy of Bruce Hart, McGill University.)

Examples of present-day workflows

Attributes used to generate sand-probability volumes

When attributes are tied to the available well control, they can be correlated to petrophysical properties, which helps the interpreter identify and associate high correlations with specific properties. For example, Figure 26 shows how attributes from prestack inversion of a high-resolution seismic data set allowed mapping of sand bodies in a geologically complex area. A key step in the workflow was the petroelastic analysis of well data which demonstrated that seismic attributes derived from prestack seismic inversion could discriminate between sands and shales.

A multiattribute-classification approach, incorporating neural-network training techniques, was used to generate sand-probability volumes derived from P-wave and S-wave impedances estimated using AVO inversion. The study demonstrated that high-resolution seismic data coupled with targeted inversion can increase confidence and reduce uncertainty in interpretation.

A crucial problem in any multiattribute analysis is the selection and the number of seismic attributes to be used. Kalkomey (1997) showed that the probability of observing a spurious correlation increases as the number of control points decreases and also as the number of seismic attributes being used increases. A way out of such a situation is to withhold a percentage of the data during the training step and then later use this hidden data to validate the predictions (Schuelke and Quirein, 1998).

Time-lapse analysis

Seismic attributes are being used effectively for time-lapse data analysis (4D). Time-lapse data analysis permits interpretation of fluid saturation and pressure changes, and helps understanding of reservoir dynamics and the performance of existing wells.

Figure 27 shows an example from east of Schiehallion field west of the Shetlands (Parr and Marsh, 2000). The preproduction surveys in 1993 (Figure 27a) and 1996 (Figure 27b) show a high degree of similarity, but the 4D survey (designed to notice changes in reservoir production) (Figure 27c) shows large changes around producers and injectors. The poor production rates and low bottom-hole-flowing pressures led to the conclusion that well C was located in a compartment that is poorly connected to injection support. The areal extent of this compartment could be picked by the amplitude increase seen on the 4D image and interpreted due to gas liberated from solution. This area is consistent with predictions from material-balance calculations.

Figure 27c from the 1999 survey suggested the possibility of a connection (marked by an arrow) between producers C and D. The existence of such a connection was also suspected from the material-balance analysis. Figure 28 shows a coherence display at the required level and depicts the expected connection (marked by the red oval). While a plausible explanation for this is not known, it is postulated that the attributes on 4D

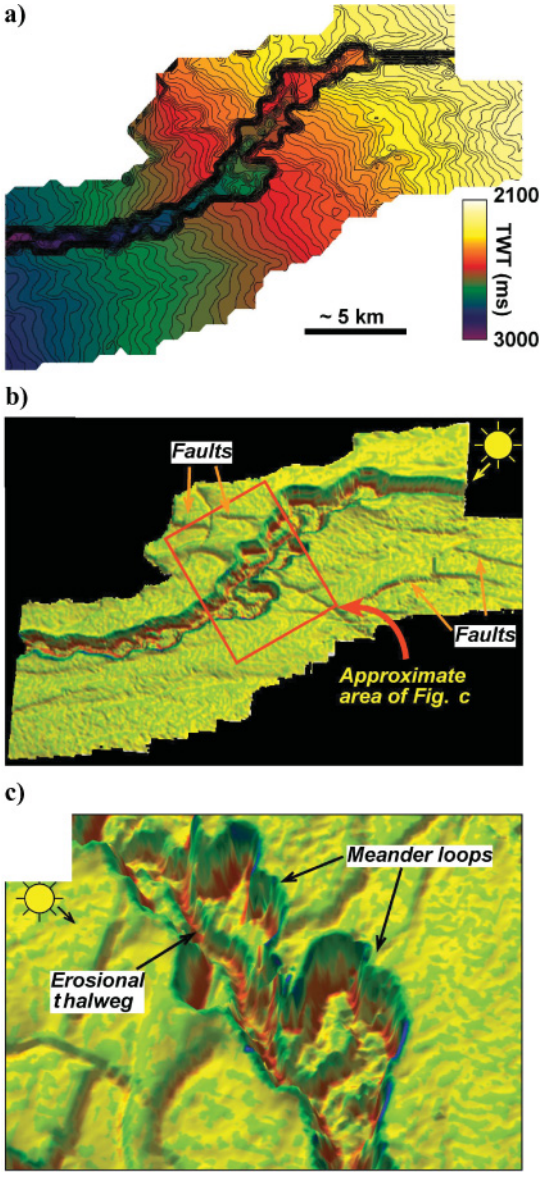

Figure 25. (a) A time-structure map of the top of a Tertiary channel-levee complex. (b) Dip component of curvature and (c) shaded relief overlain on a 3D representation of the horizon to enhance features. Note the improved definition of stratigraphic and structural features compared to the time-structure map. (Images courtesy of Bruce Hart, McGill University.)

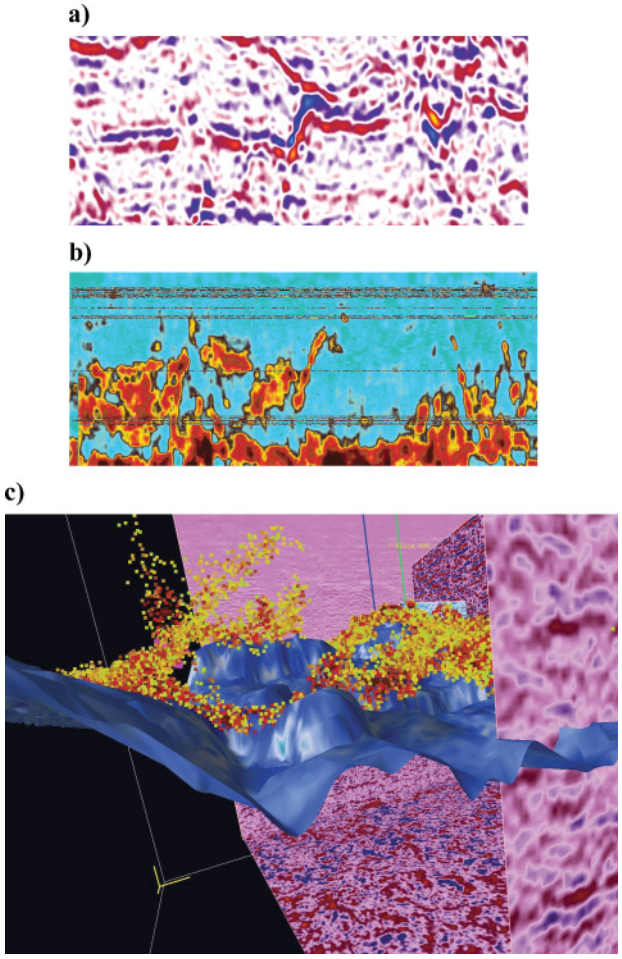

Figure 26. (a) A cross section from a final processed seismic data volume. The dipping event in the center of the panel is interpreted as a sand injection feature. (b) The same cross section from the sand-probability volume derived from multiattribute classification. The classification has predicted that the feature is sand being injected from the main sand body seen below. (c) The sand probability volume and amplitude data displayed using 3D visualization. The figure shows seismic amplitude data in the background; the base reservoir surface is shown in blue and a possible sand injection feature is mapped from the inversion results. Note the complexity of the injected sand bodies. (Images courtesy of Steve McHugo, WesternGeco.)

seismic provide a clue that a transmissibility barrier may have been broken between the injector and producer.

Reservoir-based seismic attributes are being used to help delineate anomalous areas of a reservoir where changes from time lapse are evident (Galikeev and Davis, 2005). For example, reservoir conditions caused by CO_2 injection could be detected. Attributes that represent reservoir heterogeneity are generated by computing short-time-window seismic attributes parallel to the reservoir. Such an analysis in short temporal windows ensures that the attribute carries an overprint of geology (Partyka et al., 1999).

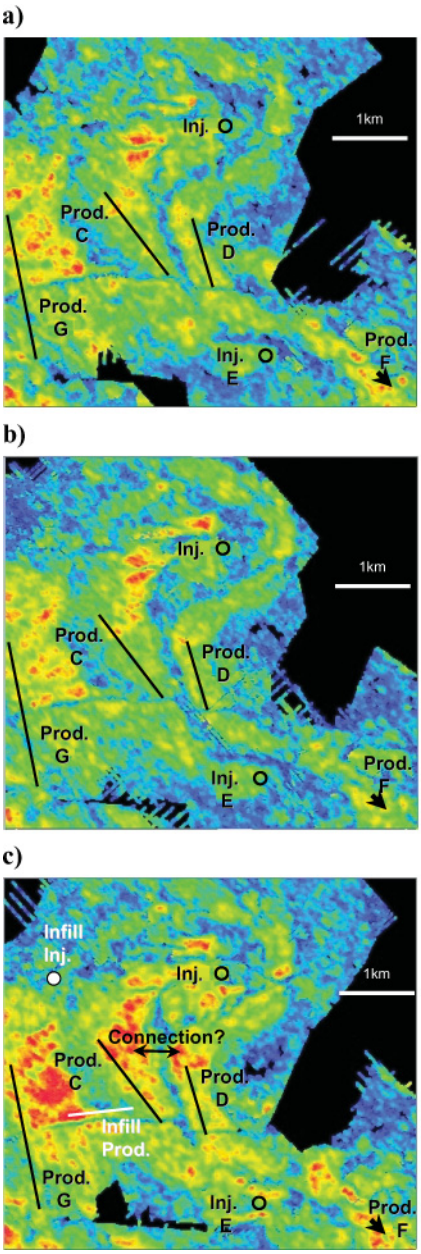

Figure 27. An example from east of Schiehallion field, west of the Shetlands. The net sand maps based on seismic amplitudes on the preproduction surveys of (a) 1993 and (b) 1996 show a high degree of similarity. Comparison with the 1999 4D survey (c) shows large changes around producers and injectors. (After Parr and Marsh, 2000.)

Figure 29 shows the dynamic changes in the Weyburn reservoir (Canada) caused by increased CO_2 saturation by computing the inverted impedance model of the reservoir on the differenced volume of the baseline (2000) and second monitor (2002) surveys. Figure 30 is a computed CO_2 saturation map, where the values do not represent absolute CO_2 saturation but rather an estimation of part porosity occupied by CO_2 after irreducible water and oil were taken into account.

Four-dimensional seismic attributes together with 4D rock and fluid analysis and incorporation of production engineering information have been used for pressure-saturation inversion for time-lapse seismic data, producing quantitative estimates of reservoir pressure and saturation changes. Application of such an analysis to the Cook reservoir of Gulfaks field, offshore Norway (Lumley et al., 2003), shows that a strong pressure anomaly can be estimated in the vicinity of a horizontal water injector, along with a strong water saturation anomaly drawing toward a nearby producing well (Figure 31). This is in addition to strong evidence of east-west fault block compartmentalization at the time of the seismic survey.

Attributes for detection of gas zones below regional velocity inversion

Evaluation of gas distribution in the fluid system in the Wind River Basin, where there are anomalously pressured gas accumulations, is a challenge. Using the available logs and seismic data, the regional velocity inversion surface has been mapped in this area (Surdam et al, 2004b), which is

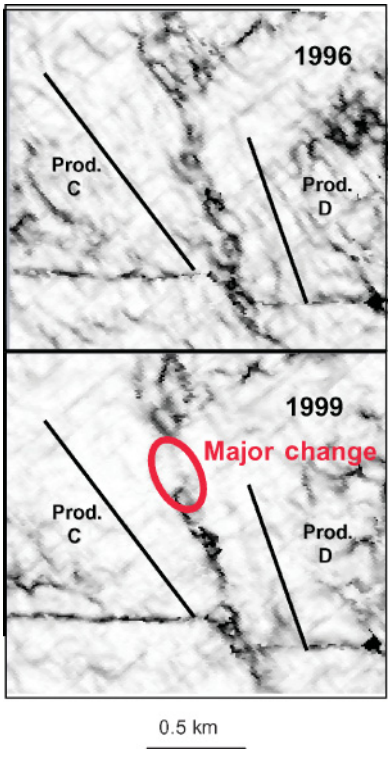

Figure 28. A time slice through a coherence volume corresponding to Figure 27. It depicts the expected connection (marked by the red oval) between producers C and D. (After Parr and Marsh, 2000).

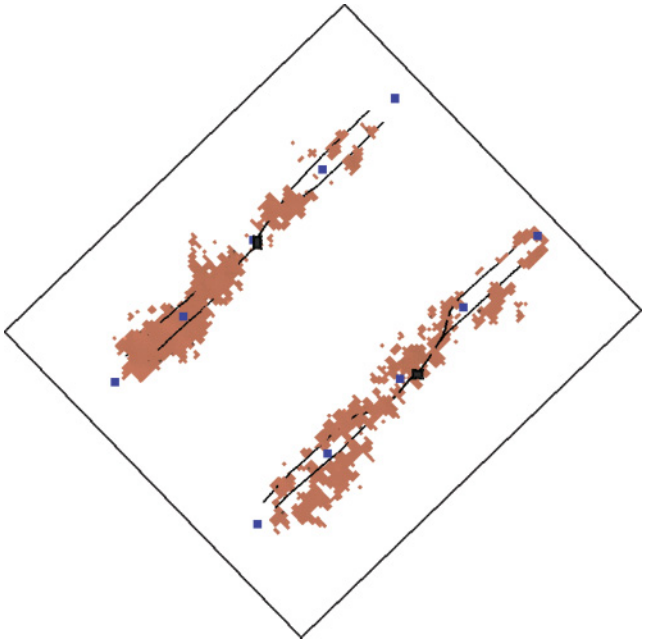

Figure 29. Position of the time-lapse impedance anomalies in depth relative to CO_2 injectors (black) and vertical water injectors (blue). The overall size of the area shown is 9 km^2. (After Galikeev and Davis, 2005.)

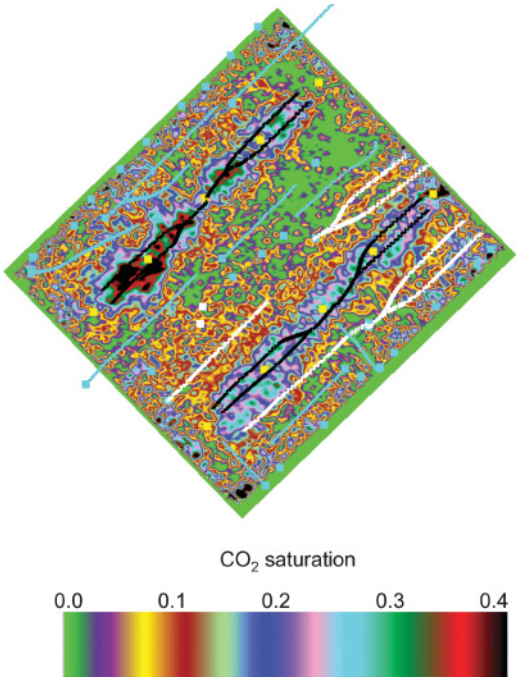

Figure 30. CO_2 saturation map computed from time-lapse (2000–2002 inversion of the difference) impedance values. Shown are areas that responded to CO_2 injection wells (white), horizontal injectors (black), unresponded to CO_2 wells (blue), and vertical water injectors (yellow). The overall size of the area shown is 9 km^2. (After Galikeev and Davis, 2005.)

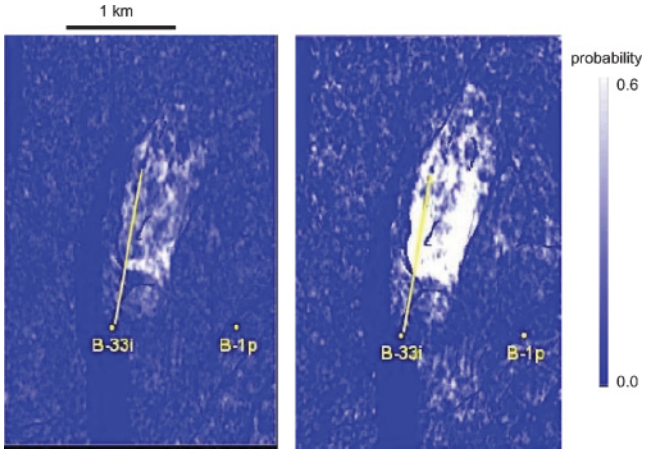

Figure 31. Probability map on a scale of zero (blue) to 0.6 (white) that water saturation (left) and pore pressure (right) have increased within the Cook reservoir of Gulfaks field, Norwegian North Sea. Note the strong pressure anomaly surrounding the B-33 horizontal injector, along with east-west sealing fault compartmentalization. Water saturation change, however, is weak in most of the compartment since well B-33 injects into the water leg. The saturation change is stronger to the southeast of the compartment where water is drawn toward nearby producing well B-1. (After Lumley et al., 2003.)

the pressure surface separating the anomalously pressured rocks below from the normally pressured rocks above. Seismic attributes have been successfully used to evaluate the distribution of sandstone-rich intervals within the prospective reservoir units. The Frenchie Draw gas field in the Wind River Basin is an example of an area where detecting and delineating gas zones below the regional velocity inversion surface is difficult. The stratigraphic interval of interest is the Upper Cretaceous–Paleocene Fort Union/Lance lenticular fluvial sandstone formations on a north-plunging structural nose. The gas distribution pattern in the formations has been found to be complex, and so the exploitation proved to be risky. Surdam (2004a) has demonstrated that a good correlation exists between seismic frequency and gamma-ray logs (lithology) in the lower Fort Union/Lance stratigraphic interval. The frequency attribute was used to distinguish sandstone-rich intervals from shale-rich intervals.

Figure 32 shows a frequency attribute section (with seismic data overlaid) covering the Fort Union/Lance stratigraphic interval intersecting the anomalously slow velocity domains (outlined by white dots). In addition to the north-plunging structural nose seen in the area, a shale-rich sequence (shown in orange) is seen near the upper edge of the gas production. Important here is the lenticular distribution of the sandstone-rich intervals in blue that stand out against the shale-rich intervals in orange and green. This distributional pattern of lithologies corresponds well with the initial interpretations carried out by geoscientists who discovered the field.

2005 AND BEYOND

The present

Active development is underway in many areas in the attribute world, and we mention here some of the prominent ones.

Volumetric estimates of curvature

Cracks or small discontinuities are relatively small and fall below seismic resolution. However, the presence of open and closed cracks is closely related to reflector curvature (since tension along a surface increases with increasing curvature and therefore leads to fracture). Until now, such curvature estimates have been limited to the analysis of picked horizons, which previously may have been affected by unintentional bias or picking errors introduced during interpretation. Volumetric curvature computation entails, first, the estimation of volumetric reflection dip and azimuth that represents the best single dip for each sample in the volume, followed by computation of curvature from adjacent measures of dip and azimuth. The result is a full 3D volume of curvature values at different scales of analysis (Al Dossary and Marfurt, personal communication, 2005).

Three-dimensional classifiers

Supervised 3D classification is being used for integrating several seismic attributes into a volume of seismic facies (Sonneland et al., 1994; Carrillat et al., 2002). Some of the most successful work is in imaging by-passed pay (Xue et al., 2003) using attributes sensitive to amplitude and trace shape. Workers at deGroot-Bril, Paradigm, Rock Solid Images, and many others have made progress in using geometric attributes as the basis for automatically picking seismic textures in 3D.

Structurally oriented filtering

Recently, several workers have used the volumetric estimates of dip and azimuth to improve the S/N ratio yet preserve discontinuities such as faults and stratigraphic discontinuities. Hoecker and Fehmers (2002) use an anisotropic diffusion algorithm that smoothes along dip azimuth only if no discontinuity is detected. Luo et al. (2002) use a multiwindow analysis technique, smoothing in the window containing the analysis point that has the smallest variance. Duncan et al. (2002) built on this latter technique, but instead of a mean filter, applied a principal-component filter in the most coherent analysis window. These structurally oriented filtering (alternatively called edge-preserving smoothing) algorithms improve not only behavior of autotrackers but also the results of coherence and other attributes sensitive to changes in reflector amplitude, waveform, and dip.

Volumetric estimation of Q

The most common means of estimating Q is through sample-by-sample estimates of spectral ratios. Typical workflows use a smoothly varying estimate of Q to increase the spectral bandwidth at depth. Most workers have focused on intrinsic versus effective Q, the latter including effects such as geometric scattering and friendly multiples. The most promising work is done with the aid of vertical seismic profiles and/or well logs. In these flows, one can interpret not only the spectral amplitude but also the spectral-phase compensation necessary to improve seismic resolution.

Prestack attributes

In addition to AVO, which measures the change in reflection amplitude and phase as a function of offset at a fixed location, we can apply attributes such as coherence and spectral decomposition to common-offset volumes to better predict changes in lithology and flow barriers. While the interpretation is entirely consistent with AVO analysis, the 3D volumes tend to show discrete geologic features and the limits of hydrocarbon distribution. There is a similar relationship between amplitude versus azimuth and geometric attributes applied to common azimuth volumes. In this latter case, we often find faults and fractures better illuminated at those acquisition azimuths perpendicular to structural trends.

Gazing into the future

Given the current data explosion both of large regional 3D surveys and also of new time-lapse and multicomponent surveys, we envision an increasingly rapid evolution of seismic attributes and computer-aided interpretation technology. Some of the clear signs on the horizon are as follows.

1) We expect continued development of texture attributes that can quantify or enhance features used in seismic stratigraphy and seismic geomorphology leading to

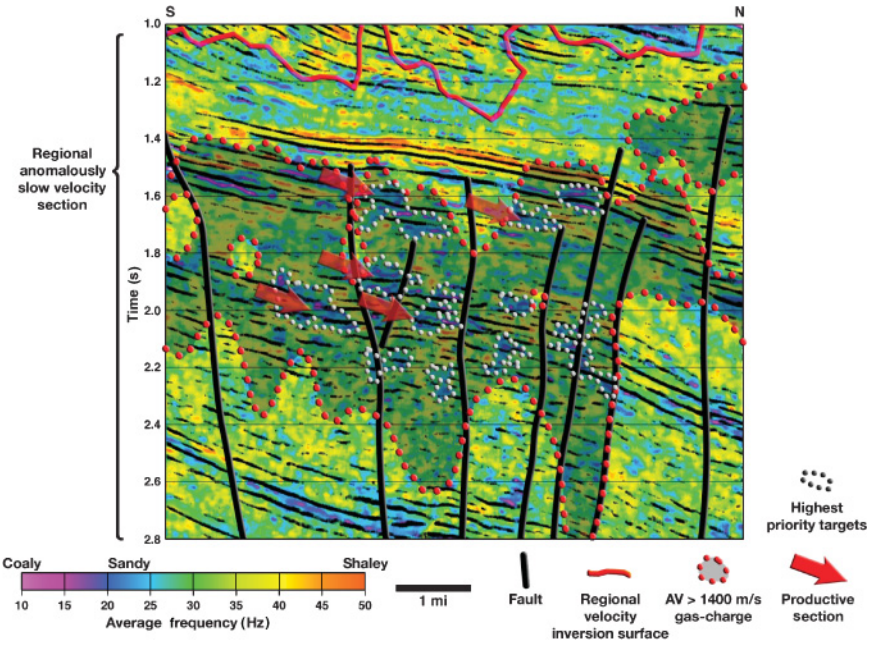

Figure 32. Seismic data display superimposed on a frequency attribute section at Frenchie Draw field, Wind River Basin. Shaded region shows anomalous velocity overlap. (After Surdam et al., 2004a.)

computer-aided 3D seismic stratigraphy. One of the major challenges is that such patterns may be arbitrarily rotated from their original position by tectonic deformation and sedimentary compaction.

2) We expect enhanced emphasis to be placed on time-lapse applications for delineation of flow-barriers, so that reservoir simulation will provide more realistic estimates and information about the dynamic behavior of reservoirs.
3) We expect continued advances in 3D visualization and multiattribute analysis, including clustering, geostatistics, and neural networks to alleviate the problems interpreters face caused by an overwhelming number of attributes.

CONCLUSIONS

A seismic attribute is a quantitative measure of a seismic characteristic of interest. Good seismic attributes and attribute-analysis tools mimic a good interpreter. Over the past decades, we have witnessed attribute developments tracking the breakthroughs in reflector acquisition and mapping, fault identification, bright-spot identification, frequency loss, thin-bed tuning, seismic stratigraphy, and geomorphology. More recently, interpreters have used crossplotting to identify clusters of attributes associated with either stratigraphic or hydrocarbon anomalies. Once again, the attribute community has worked hard to duplicate such human-driven clustering through the use of self-organized maps, geostatistics, and neural nets, and then to extend this capability beyond the three dimensions easily visualized by interpreters. Tentative steps have been taken toward computer-assisted seismic stratigraphy analysis, whereby an interpreter trains the computer on a suite of structural or depositional patterns and asks the computer to find others like them. Progress has been made in automated fault tracking, though current technology requires an expert user. In the not-too-distant future, we can envision an interpreter seeding a channel on a time slice, after which the computer paints it in 3D. Although it may take decades, we expect computers will eventually be able to duplicate all the repetitive processes performed by an interpreter. In contrast, we do not expect computers ever to replicate the creative interpreter imagining depositional environments, structural evolution, diagenetic alteration, and fluid migration. The human interpreter is here to stay but may be offshored in the future.

ACKNOWLEDGMENTS

A review paper spanning more than four decades cannot be a one- or two-man job. The authors therefore acknowledge the advice, support, and suggestions given by many prominent individuals, some of whom were actually involved in the development of the attributes in the early years.

We thank and appreciate the efforts of Nigel Anstey, Roy Lindseth, and Turhan Taner, who went down their memory lanes and provided us with their memoirs and recollections, adding greatly to our historical perspective. Nigel very graciously provided Figures 3–9, which he has treasured since 1971, and honored our request by actually writing an article entitled "Attributes in color: The early days," which has been published in the March 2005 issue of the *CSEG Recorder*. Similarly, Roy Lindseth sent us his recollections, which took the form of an article entitled "Seismic attributes — Some recollections," also published in the *CSEG Recorder*. Tury Taner encouraged us during our writing of this paper and allowed us to pick and choose from his vast selection of 35-mm slides, three of which are displayed as Figures 10–12.

A special word of appreciation goes to Jamie Robertson, who provided very useful points of view and his reminiscent write-up. We thank Alistair Brown for his advice, and we gratefully acknowledge the consultations with Brian Russell, Roy White, and Les Hatton.

Constructive comments and helpful suggestions from Sven Treitel, Bee Bednar, Jerry Schuster, and Art Barnes motivated us to include some subtle details that improved the quality of the manuscript. These are gratefully acknowledged.

Even the Professor, Bob Sheriff, not only corrected several of our historical misconceptions, but also carefully edited the entire manuscript, covering it in a sea of red ink. For some reason, the second author's students found great pleasure in this!

Finally, we thank Bruce Hart for providing Figures 24 and 25, Ronald Parr for Figures 27 and 28, Tom Davis for Figures 29 and 30, Mark Meadows for Figure 31, and Ron Surdam for Figure 32.

We have tried to cover almost all the prominent developments in this vast field of seismic attributes. However, in spite of our best efforts, it is likely we have missed out on some. Hence, any errors or omissions were unintentional and solely our responsibility.

The first author expresses his appreciation to Arcis Corporation, Calgary, for permission to use some of the data examples and to publish this paper.

REFERENCES

Anstey, N., 1973, The significance of color displays in the direct detection of hydrocarbons: 43rd Annual International Meeting, SEG.

———, 2005, Attributes in color: the early years: Canadian Society of Exploration Geophysicists Recorder, **30**, March, 12–15.

Bahorich, M. S., and S. R. Bridges, 1992, The seismic sequence attribute map (SSAM): 62nd Annual International Meeting, SEG, Expanded Abstracts, 227–230.

Bahorich, M., and P. van Bemmel, 1994, Stratigraphic interpretation of seismic data on the workstation: 64th Annual International Meeting, SEG, Expanded Abstracts, 481–484.

Bahorich, M. S., and S. L. Farmer, 1995, 3D seismic discontinuity for faults and stratigraphic features: The coherence cube: 65th Annual International Meeting, SEG, Expanded Abstracts, 93–96.

Balch, A. H., 1971, Color sonograms: A new dimension in seismic data interpretation: Geophysics, **36**, 1074–1098.

Barnes, A. E., 1996, Theory of two-dimensional complex seismic trace analysis: Geophysics, **61**, 264–272.

———, 1997, Genetic classification of complex seismic trace attributes: 67th Annual International Meeting, SEG, Expanded Abstracts, 1151–1154.

———, 2000, Attributes for automated seismic facies analysis: 70th Annual International Meeting, SEG, Expanded Abstracts, 553–556.

———, 2001, Seismic attributes in your facies: Canadian Society of Exploration Geophysicists Recorder, **26**, September, 41–47.

Batson, R. M., K. Edwards, and E. M. Eliason, 1975, Computer-generated shaded relief images: Journal of Research of the U.S. Geological Survey, **3**, 401–408.

Bednar, J. B., 2005, A brief history of seismic migration: Geophysics, **70**, 3–20MJ.

Bodine, J. H., 1984, Waveform analysis with seismic attributes: 54th Annual International Meeting, SEG, session S9.1.

———, 1986, Waveform analysis with seismic attributes: Oil and Gas Journal, **84**, no. 23, 59–63.

Brown, A. R., 1986, Interpretation of three-dimensional seismic data, 1st ed.: American Association of Petroleum Geologists Memoir 42.

———, 1996a, Interpretation of three-dimensional seismic data, 4th ed.: American Association of Petroleum Geologists Memoir 42.
———, 1996b, Seismic attributes and their classification: The Leading Edge, **15**, 1090.
———, 2004, Interpretation of three-dimensional seismic data, 6th ed.: American Association of Petroleum Geologists Memoir 42.
Brown, A. R., and J. D. Robertson, 1985, — Seismic interpretation for detailed exploration development and production: The Leading Edge, **4**, no. 10, 60–65.
Carrillat, A., T. Randen, and L. Sonneland, 2002, Seismic stratigraphic mapping of carbonate mounds using 3-D texture attributes: 64th Annual International Meeting, European Association of Geoscientists and Engineers, Z-99.
Castagna, J. P., S. Sun, and R. W. Siegfried, 2003, Instantaneous spectral analysis: Detection of low-frequency shadows associated with hydrocarbons: The Leading Edge, **22**, 120–127.
Chen, Q., and S. Sidney, 1997, Seismic attribute technology for reservoir forecasting and monitoring: The Leading Edge, **16**, 445–456.
Chopra, S., 2002, Coherence cube and beyond: First Break, **20**, no. 1, 27–33.
Chopra, S., and O. Kuhn, 2001, Seismic inversion: Canadian Society of Exploration Geophysicists Recorder: **26**, no. 1, 10–14.
Chopra, S., and D. Pruden, 2003, Multiattribute seismic analysis on AVO-derived parameters: The Leading Edge, **22**, 998–1002.
Chopra, S., V. Alexeev, and Y. Xu, 2003, 3-D AVO crossplotting — An effective visualization technique: The Leading Edge, **22**, 1078–1089.
Chopra, S., D. Pruden, and V. Alexeev, 2004, Multi-attribute seismic analysis — Tackling non-linearity: First Break, **22**, no. 12, 43–47.
Churlin, V. V., and L. A. Sergeyev, 1963, Application of seismic surveying to recognition of productive part of gas-oil strata: Geologiya Nefti I Gaza, **7**, no. 11, 363.
Claerbout, J. F., 1990, The plane-wave destructor (PWD): Stanford Exploration Project SEP-65.
Coleou, T., M. Poupon, and K. Azbel, 2003, Unsupervised seismic facies classification: A review and comparison of techniques and implementation: The Leading Edge, **22**, 942–953.
Connolly, P., 1999, Elastic impedance: The Leading Edge, **18**, 438–452.
Conticini, F., 1984, Seismic facies quantitative analysis: New tool in stratigraphic interpretation: 54th Annual International Meeting, SEG, session S18.3.
Cosentino, L., 2001, Integrated reservoir studies: Editions Technip.
Dalley, R. M., E. C. A. Gevers, G. M. Stampfli, D. J. Davies, C. N. Gastaldi, P. A. Ruijtenberg, and G. J. O. Vermeer, 1989, Dip and azimuth displays for 3-D seismic interpretation: First Break, **7**, no. 3, 86–95.
de Figueiredo, R. J. P., 1982, Pattern recognition approach to exploration, *in* R. J. P. de Figueiredo, ed., Concepts and techniques in oil and gas exploration: SEG, 267–286.
Drecun, R., and J. Lucas, 1985, Enhancement of edge patterns on horizontal time slices: 55th Annual International Meeting, SEG, Expanded Abstracts, 579–582.
Duncan, W., P. Constance, and K. J. Marfurt, 2002, Comparison of 3-D edge detection seismic attributes to Vinton Dome, Louisiana: 72nd Annual International Meeting, SEG, Expanded Abstracts, 577–580.
Ebrom, D., 2004, The low-frequency gas shadow on seismic sections: The Leading Edge, **23**, 772.
Finn, C. J., 1986, Estimation of three dimensional dip and curvature from reflection seismic data: M.S. thesis, University of Texas at Austin.
Forrest, M., 2000, "Bright" investments paid off: AAPG Explorer, July, 18–21.
Galikeev, T., and T. Davis, 2005, Time-lapse seismic attributes and reservoir volumetric calculation: 67th Annual International Meeting, European Association of Geoscientists and Engineers, Z99.
Gao, D., 2003, Volume texture extraction for 3D seismic visualization and interpretation: Geophysics, **68**, 1294–1302.
———, 2004, Texture model regression for effective feature discrimination: Application to seismic facies visualization and interpretation: Geophysics, **69**, 958–967.
Gersztenkorn, A., and K. J. Marfurt, 1999, Eigenstructure-based coherence computations as an aid to 3-D structural and stratigraphic mapping: Geophysics, **64**, 1468–1479.
Hardage, B. A., V. M. Pendleton, J. L. Simmons Jr., B. A. Stubbs, and B. J. Uszynski, 1998, 3-D instantaneous frequency used as a coherency/continuity parameter to interpret reservoir compartment boundaries across an area of complex turbidite deposition: Geophysics, **63**, 1520–1531.
Haralick, R. M., K. Shanmugam, and I. Dinstein, 1973, Textural features for image classification: IEEE Transactions, Systems, Man, and Cybernetics, SMC-3, 610–621.
Hart, B. S., R. Pearson, and G. C. Rawling, 2002, 3D seismic horizon-based approaches to fracture-swarm sweet spot definition in tight-gas reservoirs: The Leading Edge, **21**, 28–35.
Hoecker, C., and G. Fehmers, 2002, Fast structural interpretation with structure-oriented filtering: The Leading Edge, **21**, 238–243.
Kalkomey, C. T., 1997, Potential risks when using seismic attributes as predictors of reservoir properties: The Leading Edge, **16**, 247–251.
Kallweit, R. S., and L. C. Wood, 1982, The limits of resolution of zero-phase wavelets: Geophysics, **47**, 1035–1046.
Keskes, N., A. Boulanouar, Y. Lechevalier, and P. Zaccagnino, 1982, Image analysis techniques for seismic data: 52nd Annual Meeting, SEG, session S16.7.
Keskes, N., P. Zaccagnino, D. Rether, and P. Mermey, 1983, Automatic extraction of 3-D seismic horizons: 53rd Annual Meeting, SEG, session S21.1.
Knobloch, C., 1982, Pitfalls and merits of interpreting color displays of geophysical data: 52nd Annual International Meeting, SEG, session S8.8.
Landa, E., W. Beydoun, and A. Tarantola, 1989, Reference velocity model estimation from prestacked waveforms: Coherency optimization by simulated annealing: Geophysics, **54**, 984–990.
Latimer, R. B., R. Davison, and P. van Riel, 2000, An interpreter's guide to understanding and working with seismic-derived acoustic impedance data: The Leading Edge, **19**, 242–256.
Lavergne, M., 1975, Pseudo-diagraphics de Vitesse en offshore profonde: Geophysical Prospecting, **23**, 695–711.
Lindseth, R. O., 1976, Seislog process uses seismic reflection traces: Oil & Gas Journal, **74**, 67–71.
———, 1979, Synthetic sonic logs — A process for stratigraphic interpretation: Geophysics: **44**, 3–26.
———, 2005, Seismic attributes — Some recollections: Canadian Society of Exploration Geophysicists Recorder, **30**, March, 16–17.
Liner, C., C.-F. Li, A. Gersztenkorn, and J. Smythe, 2004, SPICE: A new general seismic attribute: 72nd Annual International Meeting, SEG, Expanded Abstracts, 433–436.
Lisle, R. J., 1994, Detection of zones of abnormal strains in structures using Gaussian curvature analysis: Bulletin of the American Association of Petroleum Geologists, **78**, 1811–1819.
Love, P. L., and M. Simaan, 1984, Segmentation of stacked seismic data by the classification of image texture: 54th Annual International Meeting, SEG, session S7.3.
Luo, Y., S. al-Dossary, and M. Alfaraj, 2002, Edge-preserving smoothing and applications: The Leading Edge, **21**, 136–158.
Lumley, D. Adams, M. Meadows, S. Cole, and E. Ergas, 2003, 4D seismic pressure-saturation inversion at Gulfaks field, Norway: First Break, **21**, 49–56.
Luo, Y., W. G. Higgs, and W. S. Kowalik, 1996, Edge detection and stratigraphic analysis using 3-D seismic data: 66th Annual International Meeting, SEG, Expanded Abstracts, 324–327.
Marfurt, K. J., R. L. Kirlin, S. L. Farmer, and M. S. Bahorich, 1998, 3-D seismic attributes using a semblance-based coherency algorithm: Geophysics, **63**, 1150–1165.
Marfurt, K. J., V. Sudhaker, A. Gersztenkorn, K. D. Crawford, and S. E. Nissen, 1999, Coherency calculations in the presence of structural dip: Geophysics, **64**, 104–111.
Masaferro, J. L., M. Bulnes, J. Poblet, and M. Casson, 2003, Kinematic evolution and fracture prediction of the Valle Morado structure inferred from 3-D seismic data, Salta Province, northwest Argentina: Bulletin of the American Association of Petroleum Geologists, **87**, 1083–1104.
May, B. T., and S. L. May, 1991, Elastic inversion — The key to stratigraphic interpretation: 61st Annual International Meeting, SEG, Expanded Abstracts, 1098–1101.
Meldahl, P., R. Heggland, B. Bril, and P. de Groot, 2001, Identifying faults and gas chimneys using multiattributes and neural networks: The Leading Edge, **20**, 474–478.
Okaya, D. A., 1995, Spectral properties of the Earth's contribution to seismic resolution: Geophysics, **60**, 241–251.
Parr, R. S., and M. Marsh, 2000, Development of 4-D reservoir management West of Shetland: World Oil, Sept. 39–47.
Partyka, G., J. Gridley, and J. Lopez, 1999, Interpretational applications of spectral decomposition in reservoir characterization: The Leading Edge, **18**, 353–360.
Payton, C. E., ed., 1977, Seismic stratigraphy — Applications to hydrocarbon exploration: American Association of Petroleum Geologists Memoir 26.
Peterson, R. A., W. R. Fillippone, and F. B. Coker, 1955, The synthesis of seismograms from well log data: Geophysics, **20**, 516–538.
Peyton, L., R. Bottjer, and G. Partyka, 1998, Interpretation of incised valleys using new 3-D seismic techniques: A case history using spectral decomposition and coherency: The Leading Edge, **17**, 1294–1298.

Picou, C., and R. Utzmann, 1962, La coupe sismique vectorielle: Un pointé semi-automatique: Geophysical Prospecting, **4**, 497–516.
Ravenne, C., 2002, Stratigraphy and oil: A review, Part 1: Exploration and seismic stratigraphy: Observation and description: Revue de l'Institute Français du Pétrole, **57**, 211–250.
Rijks, E. J. H., and J. C. E. M. Jauffred, 1991, Attribute extraction: An important application in any detailed 3D interpretation study: The Leading Edge, **10**, 11–19.
Roberts, A., 2001, Curvature attributes and their application to 3-D interpreted horizons: First Break, **19**, no. 2, 85–99.
Robertson, J. D., and D. A. Fisher, 1988, Complex seismic trace attributes: The Leading Edge, **7**, no. 6, 22–26.
Robertson, J. D., and H. H. Nogami, 1984, Complex seismic trace analysis of thin beds: Geophysics, **49**, 344–352.
Rummerfeld, B., 1954, Reflection quality, a fourth dimension: Geophysics, **19**, 684–694.
Russell, B., D. Hampson, J. Schuelke, and J. Quirein, 1997, Multiattribute seismic analysis: The Leading Edge, **16**, 1439–1443.
Sangree, J. B., and J. M. Widmier, 1976, Seismic interpretation of clastic depositional facies: American Association of Petroleum Geologists Memoir 26, 165–184.
Scheuer, T. E., and D. W. Oldenberg, 1988, Local phase velocity from complex seismic data: Geophysics, **53**, 1503–1511.
Schuelke, J. S., and J. A. Quirein, 1998, Validation: A technique for selecting seismic attributes and verifying results: 68th Annual International Meeting, SEG, Expanded Abstracts, 936–939.
Sheriff., R. E., comp., 1984, Encyclopedic dictionary of exploration geophysics, 2nd ed.: SEG.
———, comp., 1991, Encyclopedic dictionary of exploration geophysics, 3rd ed.: SEG.
———, comp., 2002, Encyclopedic dictionary of applied geophysics, 4th ed.: SEG, Geophysical References Series 13.
Sibille, G., N. Keskes, L. Fontaine, and J. L. Lequeux, 1984, Enhancement of the perception of seismic facies and sequences by image analysis techniques: 54th Annual International Meeting, SEG, session S7.2.
Sigismondi, M., and J. C. Soldo, 2003, Curvature attributes and seismic interpretation: Case studies from Argentina basins: The Leading Edge, **22**, 1122–1126.
Simpson, S. M., D. Fink, and S. Treitel, 1967, Moveout averaging experiments: Geophysics, **32**, 494–498.
Sonneland, L., O. Barkved, M. Olsen, and G. Snyder, 1989, Application of seismic wave-field attributes in reservoir characterization: 59th Annual International Meeting, SEG, Expanded abstracts, 813.
Sonneland, L., P. Tennebo, T. Gehrmann, and O. Yrke, 1994, 3-D model-based Bayesian classification: 64th Annual International Meeting, SEG, Expanded Abstracts, 510–511.
Stewart, S. A., and T. J. Wynn, 2000, Mapping spatial variation in rock properties in relationship to scale-dependent structure using spectral curvature: Geology, **28**, 691–694.
Surdam, R. C., Z. S. Jioa, and Y. Ganshin, 2004a, Reducing risk in low-permeability gas formations: Understanding the rock fluid characteristics of Rocky Mountain Laramide basins: DOE Final Technical Progress Report under contract no. DE-FC26-01NT41325, 39.
———, 2004b, Reducing the risk of exploring for anomalously pressured gas assets: GasTIPS, **10**, no. 4, 4–8
Taner, M. T., 2001, Seismic attributes: Canadian Society of Exploration Geophysicists Recorder, **26**, no. 9, 48–56.
Taner, M. T., and R. E. Sheriff, 1977, Application of amplitude, frequency, and other attributes to stratigraphic and hydrocarbon determination, *in* C. E. Payton, ed., Applications to hydrocarbon exploration: American Association of Petroleum Geologists Memoir 26, 301–327.
Taner, M. T., F. Koehler, and R. E. Sheriff, 1979, Complex seismic trace analysis: Geophysics, **44**, 1041–1063.
Taner, M. T., J. S. Schuelke, R. O'Doherty, and E. Baysal, 1994, Seismic attributes revisited: 64th Annual International Meeting, SEG, Expanded Abstracts, 1104–1106.
Taner, M. T., D. E. Wagner, D. E. Baysal, and L. Lu, 1998, A unified method for 2-D and 3-D refraction statics: Geophysics, **63**, 260–274.
Thadani, S. G., F. Aldabert, and A. G. Journel, 1987, An integrated geostatistical/pattern recognition technique for characterization of reservoir spatial variability: 57th Annual International Meeting, SEG, session SEG 1.2.
Vail, P. R., R. M. Mitchum Jr., and S. Thompson III, 1977, Seismic stratigraphy and global changes of sea level, Part 4: Global cycles of relative changes of sea level, *in* C. E. Payton, ed., Seismic stratigraphy applications to hydrocarbon exploration: American Association of Petroleum Geologists Memoir 26, 83–97.
Verm, R. W., and F. J. Hilterman, 1994, Lithologic color-coded sections by AVO crossplots: 64th Annual International Meeting, SEG, Expanded Abstracts, 1092–1095.
Vinther, R., 1997, Seismic texture classification applied to processed 2-D and 3-D seismic data: 67th Annual International Meeting, SEG, Expanded Abstracts, 721–724.
Vinther, R., K. Mosegaard, K. Kierkegaard, I. Abatzis, C. Andersen, O.Vejback, F. If, and P. Nielsen, 1995, Seismic texture classification: A computer-aided approach to stratigraphic analysis: 65th Annual International Meeting, SEG, Expanded Abstracts, 153–155.
Vossler, D. A., 1988, Automatic whole section seismic reflection mapping: 58th Annual International Meeting, SEG, session S2.2.
West, B., S. May, J. E. Eastwood, and C. Rossen, 2002, Interactive seismic facies classification using textural and neural networks: The Leading Edge, **21**, 1042–1049.
Whitcombe, D. N., 2002, Elastic impedance normalization: Geophysics, **67**, 60–62.
White, R. E., 1991, Properties of instantaneous seismic attributes: The Leading Edge, **10**, no. 7, 26–32. Discussion and reply in **11**, no. 8, 45–46 and **11**, no. 10, 10–12.
Whitehead, P., J. Fairborn, and R. Wentland, 1999, Identifying stratigraphic units by seismic patterns, 69th Annual International Meeting, SEG, Expanded Abstracts, 942–945.
Xue, F., D. Paddock, K. Hemsley, 2003, 3D seismic classification — An efficient approach for prospect identification in asset evaluation: 73rd Annual International Meeting, SEG, Expanded Abstracts, 1485–1488.